EUROPEAN ORGANIZATION FOR NUCLEAR RESEARCH

CERN-PPE/93-08

25 January 1993

THE RENAISSANCE OF EXPERIMENTAL NEUTRINO PHYSICS

Carlo Rubbia

CERN, CH-1211 Geneva 23, Switzerland

Presented at the Conversaciones de Madrid

El Escorial, Madrid, Spain

September 5, 1992

CONTENTS

1 OPENING REMARKS

It is a great pleasure for me to be in Madrid once again, especially during this 'Year of Spain' with Barcelona and Seville hosting international events, and with Madrid as the European Cultural Capital. I would like to extend my warmest thanks to the organizers of Conversaciones de Madrid for giving me this opportunity to participate in these discussions on High-Energy Physics and Cosmology.

May I also congratulate your choice of El Escorial for this conference. Its magnificent palace is a living witness to the glorious cultural history of Spain, and it is my sincere hope that the scientific future of Spain will prove to be equally rewarding.

Turning to the main point for discussion today, let me try to paint the picture of one of the most mysterious areas of particle physics, the neutrinos, which are the object of a true revolution and which promise to bring us the answers to questions on extraordinary issues reaching far beyond the specific world of elementary particles.

2 NEUTRINO MASSES

2.1 Neutrinos as elementary particles

Neutrinos constitute one of the building blocks of matter. Classified as leptons, they are what physicists call 'elementary particles'.

An elementary particle, in the time-honoured sense of the term, is structureless and indivisible, although history cautions that the physicist's list of elementary particles is dependent upon experimental resolution, and thus subject to revision with the passage of time. We thus have no experimental reason, but only tradition, to suspect that today's elementary particles might not be the ultimate elementary particles.

In some sense our present theory, the Standard Model, is very complicated. It contains too many arbitrary parameters and nobody believes that it could be the 'ultimate theory'. In the Standard Model, neutrinos are massless, and if one had good reasons to believe that it should indeed be the case, that Nature had compelling reasons for assigning a vanishing mass to those particles, I would probably not be discussing today 'The Renaissance of Experimental Neutrino Physics'. Fortunately, the very reasons which induce us to think that there must be some new fundamental physics which lies behind the so-called 'Standard Model' and explains some of its 'arbitrary' features, also lead us to suspect that neutrinos have a mass, however small

it might be. In fact, the general prejudice today among physicists is that neutrinos do have a mass (m_ν), which may be very small but not zero.

The 'see-saw' models [1] provide a reasonable extension of the Standard Model. Neutrino masses in such models originate from couplings that they have with partners that are right-handed Majorana neutrinos, too heavy to be observed. The mass terms in the Lagrangian are written as [2] :

$$(m_D\,\overline{\nu}_L N_R + \frac{1}{2} M_N \overline{N}_L^C N_R) = \frac{1}{2}\left(\overline{\nu}_L, \overline{N}_L^C\right)\begin{bmatrix} 0 & m_D \\ m_D^T & M_N \end{bmatrix}\begin{pmatrix} \nu_R^C \\ N_R \end{pmatrix}$$

where ν is a Dirac and N a Majorana neutrino. For Dirac-type neutrinos, neutrinos and antineutrinos are different particles; in the Standard Model neutrinos exist only in a negative helicity state while antineutrinos exist only in a positive helicity state. For Majorana neutrinos, the neutrino and the antineutrino are the same particle, but that particle exists in two different helicity states, interacting differently with matter. If one allows three flavours, each entry in the above mass matrix is a 3×3 matrix. By diagonalization of the mass matrix, three light left-handed Majorana neutrinos (corresponding to the observed ν_e, ν_μ, ν_τ) and three superheavy Majorana neutrinos (corresponding to unobserved massive particles) are generated.

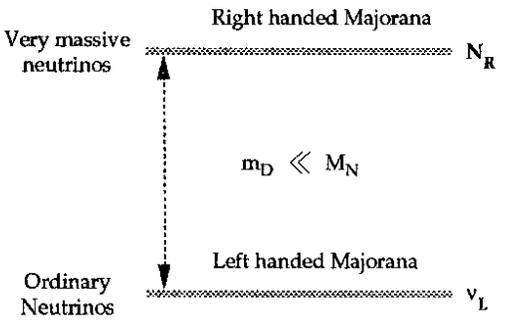

Figure 1 : Mass splitting between left-handed and right-handed Majorana neutrinos.

Assuming that the eigenvalues of M_N are much greater than those of m_D (Figure 1), the light neutrinos acquire a mass $m_\nu = m_D M_N^{-1} m_D^T$ that, in the limit when M_N is proportional to the identity matrix, is given by a quadratic see-saw: $m_\nu \approx m_D^2 / M_N$. In the type of model considered here, both quarks and leptons are expected to have masses of order m_D. If all masses are evaluated at the GUT scale M_X, neglecting family mixing, one obtains for each family: $m_{\nu_i}(X) = m_{D_i}^2(X) / M_{N_i}(X)$. All the masses involved then have to be run down to the relevant low-energy scale by means of the renormalization group calculation. Note that variants of these models can also result in linear see-saw mechanisms, if for instance the eigenvalues of M_N follow the same hierarchy as M_D.

In conclusion one can say that we do understand the smallness of neutrino masses to some extent from the fact that the $M_{N_i}(X)$ terms are very large. However, we do not know whether m_{D_3} is proportional to m_{top} or m_τ and whether we should use a quadratic or a linear see-saw mechanism. Taking the ratio of neutrino masses eliminates the overall unknown mass scale $M_{N_i}(X)$. Assuming we know the muon neutrino (ν_μ) mass, we can compute the tau neutrino (ν_τ) mass, modulo radiative corrections! As an instructive exercise, we can for instance consider the case m_{ν_μ} = 0.5 milli-electronvolt and study the corresponding ν_τ mass ranges for different assumptions (Table 1):

Table 1

m_{ν_τ} (eV)	Quadratic see-saw	Linear see-saw
with quarks	2 ~ 12	0.03 ~ 0.08
with leptons	0.14	0.009

With these models, one obtains typically $m_{N_2} = 2 \times 10^{10}$ or 3×10^{12} GeV, depending on whether one uses a quadratic or linear see-saw mechanism with leptons or with quarks. The scale for m_N must come from the breaking of some symmetry (e.g. Peccei-Quinn). A more definite theory is needed to provide clear predictions. Many models exist to extend the Standard Model, let us now take some specific examples in order to have a better idea of magnitudes for neutrino masses.

2.2 Neutrino masses in the Supersymmetric Grand Unified Theory (SUSY GUT)

This model [3] requires a unification scale M_X of $1.6 \times 10^{16\pm0.4}$ GeV and a SUSY symmetry breaking scale smaller than or equal to about 1 TeV, consistent with the recent LEP data. The neutrino masses are given by a quadratic see-saw mechanism using quark masses:

$$m_{\nu_e} = (0.05)\frac{m_u^2}{M_N} < 2 \times 10^{-11} eV$$

$$m_{\nu_\mu} = (0.09)\frac{m_c^2}{M_N} = 6 \times 10^{-9} \div 4 \times 10^{-6} eV$$

$$m_{\nu_\tau} = (0.38)\frac{m_t^2}{M_N} = 0.00011 \div 0.87 eV$$

The uncertainties are due mainly to the errors on M_N and m_t. In this scenario the masses are too small to play an important cosmological role, such as providing the matter needed to close our Universe.

2.3 Neutrino masses in the non-Supersymmetric SO(10) Grand Unified Theory

In this model [4], a first symmetry breaking down to a Left-Right symmetric model occurs at the GUT scale $M_X = 9.6 \times 10^{16\pm0.4}$ GeV, followed by a second symmetry breaking down to the Standard Model at an intermediate energy scale $M_R = 1.5 \times 10^{10\pm0.3}$ GeV. The corresponding value for M_N is $(0.01 \div 1)M_R = (7.5 \times 10^7 \div 3 \times 10^{10})$ GeV. With these values of the relevant parameters one obtains:

$$m_{\nu_e} = (0.05)\frac{m_u^2}{M_N} < 2 \times 10^{-5} eV$$

$$m_{\nu_\mu} = (0.07)\frac{m_c^2}{M_N} = 5 \times 10^{-3} \div 2.2\ eV$$

$$m_{\nu_\tau} = (0.18)\frac{m_t^2}{M_N} = 60 \div 10^5 eV$$

The range of values for the tau neutrino mass must be compared to the cosmological upper limit which is 28 eV [5]! This is a major constraint which this model has to take into account. The general feature that one might want to retain of all this discussion is that quadratic see-saw models provide a natural mass hierarchy for neutrinos:

$$m_{\nu e} : m_{\nu \mu} : m_{\nu \tau} = m_u^2 : m_c^2 : m_t^2$$

This implies that in terms of cosmological effects only the tau neutrino counts. If the tau neutrino mass happened to be around $10 \div 20$ eV, it would be very exciting since it would mean that neutrinos are closing the Universe and that they are the most abundant type of matter in the Universe.

3 MIXING OF NEUTRINO SPECIES

After having discussed the possibility that neutrinos have a mass, the next natural issue is that of mixing among neutrino flavours. Although there is no compelling reason why neutrino families should mix like quarks do, it is very likely that 'some' mixing occurs also in the neutrino sector. Mixing among neutrino species is a way to express that the weak interaction eigenstates, for instance ν_e and ν_μ, are different from the mass eigenstates ν_1 and ν_2. The standard formalism introduces a mixing matrix similar to the quark mixing matrix which, for the simplifying case of only two neutrino species, is written as:

$$\begin{pmatrix} \nu_e \\ \nu_\mu \end{pmatrix} = \begin{bmatrix} \cos(\theta) & \sin(\theta) \\ -\sin(\theta) & \cos(\theta) \end{bmatrix} \begin{pmatrix} \nu_1 \\ \nu_2 \end{pmatrix}$$

There is also no known reason why neutrino mixing parameters should emulate the quark Cabbibo–Kobayashi–Maskawa matrix, but if they do, then we would have the following scenario:

$$\sin^2 2\theta_{e\mu} = 0.18; \qquad \sin^2 2\theta_{\mu\tau} = 0.004 \div 0.012; \qquad \sin^2 2\theta_{e\tau} = 1.6 \times 10^{-5} \div 2 \times 10^{-4}$$

It is my own personal prejudice that the actual angles are going to be quite a bit smaller than those for quarks. However, if the texture of the neutrino mixing matrix follows the one for quarks, then on rather general grounds one expects: $\theta_{\mu\tau} \sim \theta_{e\mu}^2$ and $\theta_{e\tau} \sim \theta_{e\mu}^3$ which implies: $\theta_{e\tau} << \theta_{\mu\tau} << \theta_{e\mu}$. The best conclusion for the elementary particle physics point of view is that masses and angles are likely to be very small but there is a definite hierarchy between them. This is probably a very valuable hint.

4 NEUTRINO MASSES AND COSMOLOGY

Our confidence in nucleosynthesis has gained credibility now that its indication of three or four neutrino families has been vindicated by the LEP result : $N_\nu = 3.04 \pm 0.04$ [6]. The amount of baryonic matter in the Universe inferred by our nucleosynthesis model is by far too low to close the Universe. The type of Universe we are living in depends on the relation between $\bar{\rho}$, its mean density and $\rho_c = 3H_0^2/8\pi G = 1.879 \times 10^{-29}\ h^2\ g/cm^3$, the critical density. G is the gravitational constant, H_0 the Hubble constant and h is defined from $H_0 = h \times 100$ km s^{-1}/Mpc. The present data imply $0.5 < h < 1$. It is convenient to introduce Ω, the ratio of the mean density to the critical density: $\Omega \equiv \rho/\bar{\rho}$. If $\Omega > 1$, the Universe is closed. However, the baryonic matter contribution to Ω, Ω_B is found to be at most 0.07, which is far too small to close the Universe.

Many cosmologists believe that $\Omega = 1$ to high accuracy. Reasons for this belief include the inflation hypothesis [7] which (a) resolves several traditional problems with the Friedmann–Robertson–Walker cosmological model (for which the Universe is homogeneous and isotropic on sufficiently large scales) and (b) predicts $\Omega = 1$.

If $\Omega = 1$ and $\Omega_B < 0.07$, a large additional quantity of 'dark' matter must exist and it is generally accepted that it consists of both 'hot' (HDM) and 'cold' (CDM) components. The recent COBE observations [8] on the large-scale structure of the Universe have indicated a possible sharing: $\Omega_{HDM} \sim 0.3$ and $\Omega_{CDM} \sim 0.7$. Among the Hot Dark Matter candidates, neutrinos seem to be the most credible option, while for

Cold Dark Matter many possibilities are considered including SUSY photinos, exotic massive particles, baryonic dark matter (MACHO), etc.

It is therefore a very plausible cosmological hypothesis that neutrinos constitute a significant fraction of dark matter. With the mass hierarchy discussed above, one neutrino species dominates entirely and the closure condition for the Universe is simply: $m_{\nu\tau} = 91.5\ \Omega_\nu h^2$ (eV). This in turn sets a definite window for $m_{\nu\tau}$, for the heaviest of the three types of neutrinos: $6.8\ \text{eV} \leq m_{\nu\tau} \leq 27.5\ \text{eV}$.

I would now like to discuss the experimental implications of such mass scales, in other words, how can we experimentally determine such a neutrino mass?

5 NEUTRINO MASSES AND OSCILLATIONS: 'KILL TWO BIRDS WITH ONE STONE'

Any plausible cosmological limit for neutrino masses puts their determination outside present-day elementary particle physics capabilities, with maybe the exception of ν_e. However, even for ν_e, present limits from neutrinoless double β-decay probably already exclude masses of interest. Moreover, generally only ν_τ or possibly ν_μ are considered serious candidates for Hot Dark Matter (mass hierarchy). Unfortunately, for these species, well-established kinematic properties make direct measurements of their masses, $m_{\nu\tau}$ and $m_{\nu\mu}$, impossible for the interesting mass range. However we are fortunate that other methods exist, indirect measurements through neutrino mixing, which offer us a unique window for the observation of such very small neutrino masses.

Experimentally one observes conversion in vacuum between neutrino flavours after a sufficiently long path L related to the difference between the two mass eigenstates squared : $\Delta m^2 = m_2^2 - m_1^2$. To gain insight into the mechanism it is sufficient to consider the case of two families, where one can calculate simply the probability of conversion of ν_1 into ν_2: $P(\nu_1 \rightarrow \nu_2) = \sin^2(2\theta) \sin^2(\pi L/\ell_\nu)$, where $\ell_\nu = 4\pi P/\Delta m^2 = 2.48\ P\ (\text{MeV})/\Delta m^2\ (\text{eV}^2)$ if ℓ_ν is expressed in metres. If neutrino oscillations were observed, it would be evidence for non-zero neutrino masses, hence the increased importance of searching for such a phenomena.

6 THE 'SAGA' OF THE SOLAR NEUTRINO PUZZLE

The strong yield of neutrinos from the sun which is expected to produce as many as 10^{10} neutrinos/cm^2/s on the earth's surface, and the huge distance sun–earth (149×10^6 km!) make the sun an ideal tool to study neutrino oscillations. The

only known potentially better tool is provided by supernovae, but their rate is unfortunately very small. The present situation on solar neutrinos is the result of four well-known key experiments.

6.1 Experimental results

6.1.1 Homestake

The Homestake radiochemical chlorine solar neutrino detector [9] (Figure 2) built during the period 1965–67 in the Homestake Gold Mine at Lead, South Dakota, USA is the pioneering experiment led by R. Davis. The method is based upon the inverse β-decay process: $\nu_e + {}^{37}Cl \rightarrow {}^{37}Ar + e^-$, for which the neutrino energy threshold is $E_\nu = 814$ keV. The reaction used is sensitive to ^7Be and ^8B neutrinos produced in the core of the sun (Figure 3). The physical target consists of 615 tons of perchloroethylene, corresponding to 2.3×10^{30} atoms of ^{37}Cl.

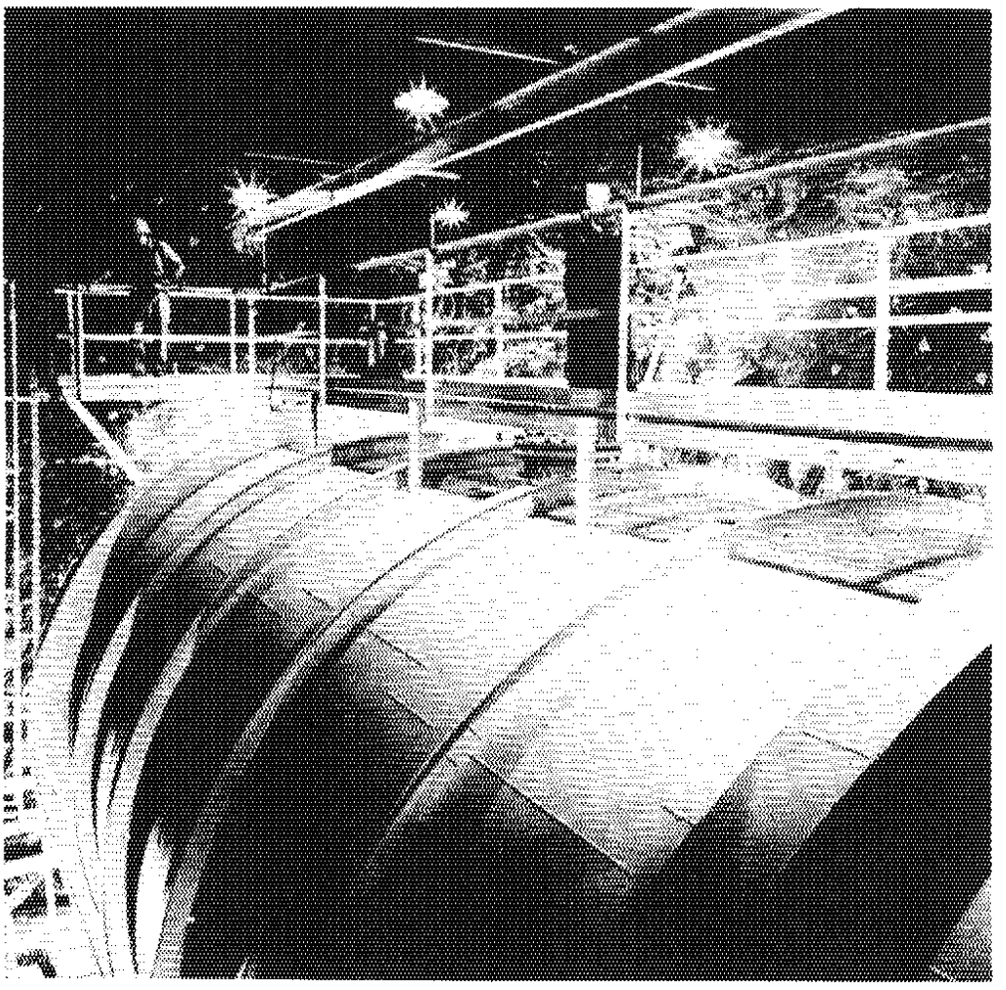

Figure 2 : Photograph of the Homestake detector.

The location in a deep underground mine eliminates the main background: $p + {}^{37}Cl \rightarrow {}^{37}Ar + n$, which, with the natural rock shielding, is reduced to only 1.5 ^{37}Ar atoms per day! The detection method for ^{37}Ar uses atomic X rays from the K capture of an electron: $e^- + {}^{37}Ar \rightarrow \nu_e + {}^{37}Cl$, for which the lifetime is $\tau_{1/2} \sim 34$ days (Figure 4). The experiment has now been producing results [10] (Figure 5) for more than 20 years!

While the Standard Solar Model (SSM) predicts a rate of 8.0 ± 3.0 SNU (Bahcall) [11] and 6.4 ± 1.4 SNU (Turck-Chièze) [12], the Homestake result is 2.2 ± 0.2 SNU where one SNU is defined as one capture per second per 10^{36} target atoms. It came as a big surprise that the rate of neutrinos coming from the sun was apparently smaller than expected by a rather large factor.

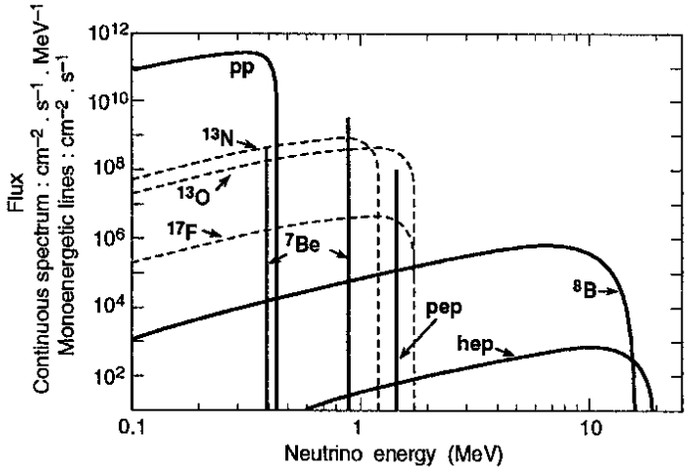

Figure 3 : Solar Neutrino Energy Spectrum.

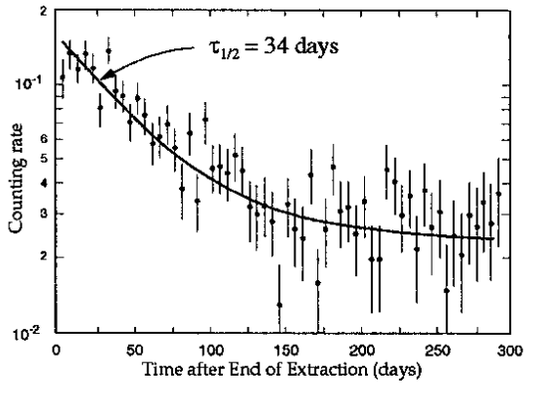

Figure 4 : Counting rate in proportional counters after extraction of ^{37}A from Homestake, showing the expected half life of 34 days.

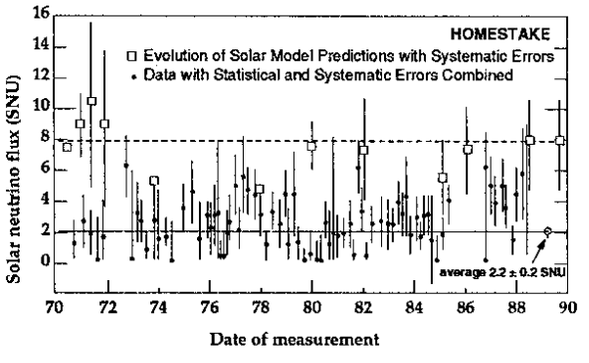

Figure 5 : Homestake solar neutrino flux measurement over a period of 20 years.

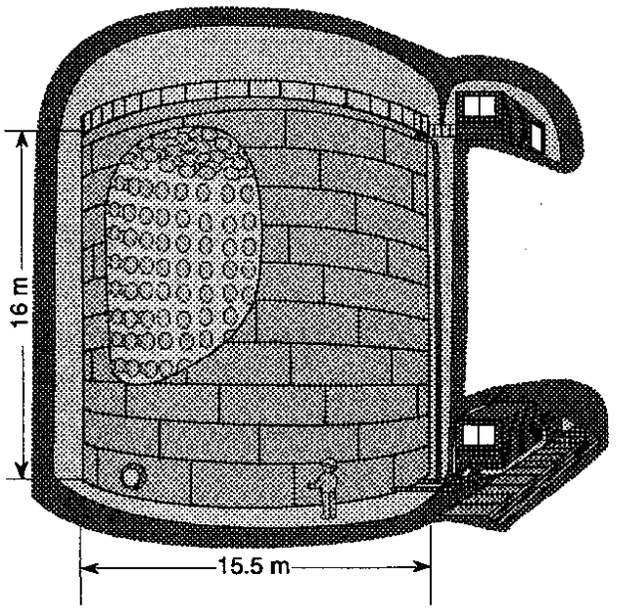

Figure 6a: Schematics of the Kamiokande Detector.

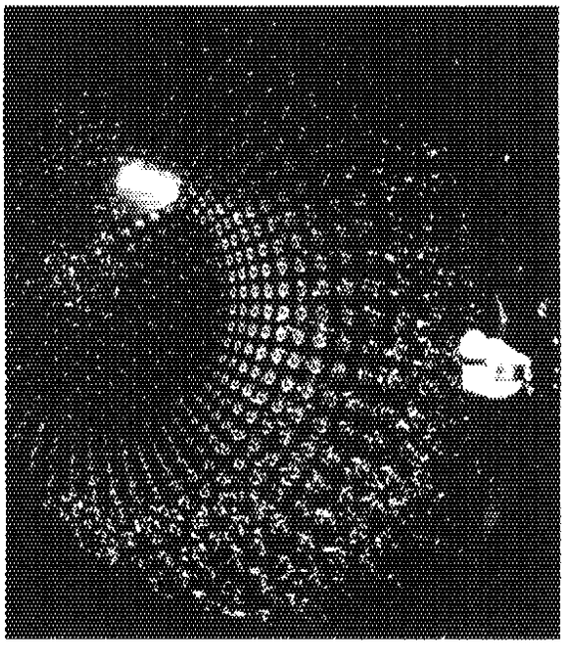

Figure 6b : Photograph of Kamiokande Detector, showing the array of 948 photomultiplier tubes.

6.1.2 Kamiokande

Kamiokande, a 'real-time' experiment [13], in the Kamioka Mine in Japan, has confirmed the surprising result from Homestake. The experiment consists in detecting, with 948 photomultiplier tubes (Figure 6 a & b), Cherenkov light produced in 680 tons of water by the electrons from the reaction: $\nu_e + e^- \rightarrow \nu_e + e^-$. The electron energy threshold of 7.5 MeV implies that the experiment is only sensitive to ^8B neutrinos at the upper end of the expected energy spectrum of solar neutrinos. The experiment also provides some sensitivity to $\nu_{\mu,\tau} + e^- \rightarrow \nu_{\mu,\tau} + e^-$ for which the cross-section is about 20% of the ν_e cross-section. There is a useful directional correlation between the detected electron and the incident neutrino (Figure 7).

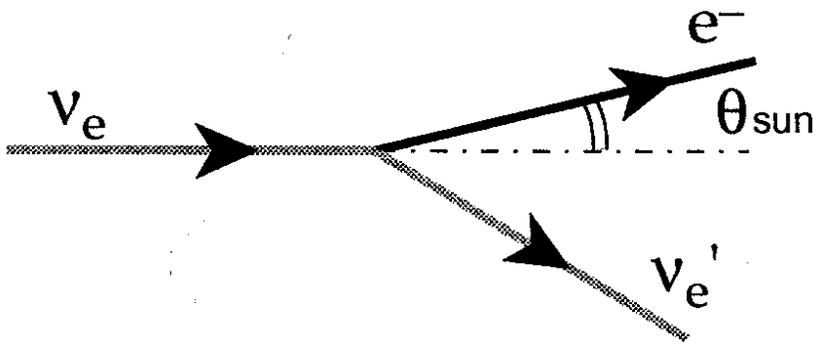

Figure 7 : Definition of θ_{sun} the angle between the scattered electron and the initial solar neutrino direction.

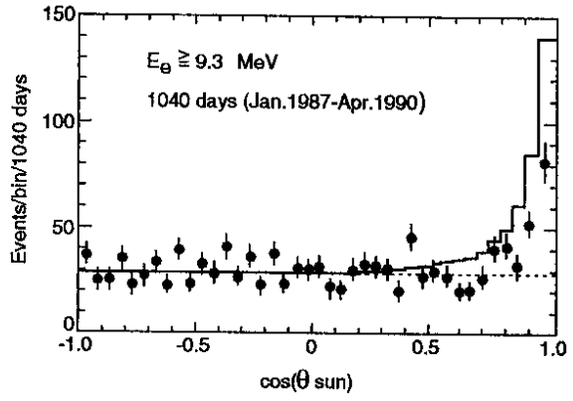

Figure 8a : Angular distribution of neutrino events producing an electron in Kamiokande with $E_e \geq 9.3$ MeV.

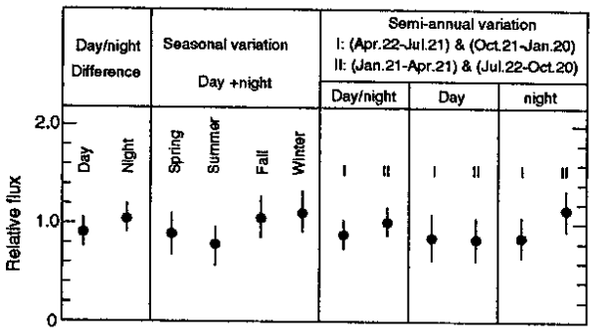

Figure 8b : Day-night and seasonal variation of solar neutrino flux in Kamiokande.

Indeed the data show a clear signal in the direction of the sun (Figure 8 a & 9 a). No significant time variation of the signal is found (Figures 8 b and 9 b). The magnitude of the experimental signal compared to the prediction of solar models is [14] :

$$\text{Data/Theory} = 0.47 \pm 0.05 \pm 0.06 \text{ (Bahcall)}$$

$$0.61 \pm 0.06 \pm 0.13 \text{ (Turck-Chièze)}$$

which confirms the existence of a solar neutrino deficit as first observed by of the Homestake experiment.

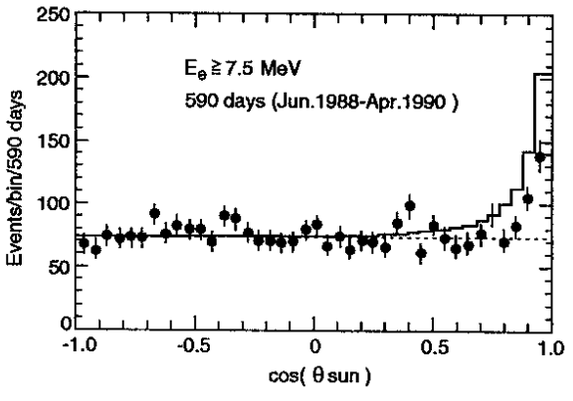

Figure 9a : Angular distribution of neutrino events producing an electron in Kamiokande with $E_e \geq 7.5$ MeV.

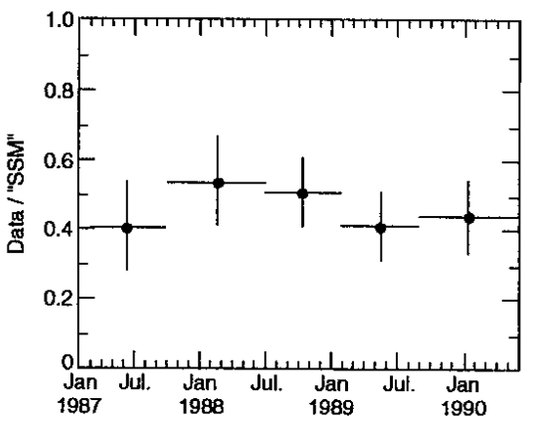

Figure 9b : Variation with time of the relative rate of events in Kamiokande with respect to the Standard Solar Model prediction.

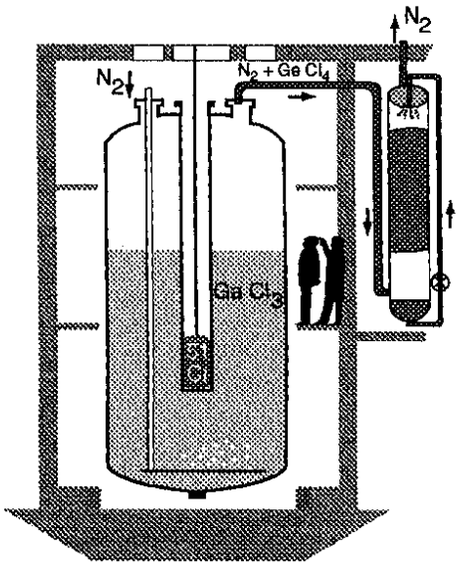

Figure 10 : Schematics of the ^{71}Ge extraction in Gallex.

6.1.3 GALLIUM EXPERIMENTS

The third type of solar neutrino experiments are radiochemical detectors using gallium – one of them is SAGE (Soviet American Gallium Experiment) [15] in an underground laboratory under Mount Andyrchi in the Baksan Valley in the Northern Caucasus, which uses 60 tons of natural gallium. The other one is GALLEX [16] using 30.7 tons of gallium containing 12 tons of ^{71}Ga. Both experiments use the reaction: $\nu_e + {}^{71}Ga \rightarrow e^- + {}^{71}Ge$, for which the neutrino energy threshold of only 233 keV allows sensitivity to the basic pp process inside the sun. Gallex is situated deep underground in the Gran Sasso tunnel to eliminate the cosmic ray background. It is expected that the background at the location of the detector is smaller than one ^{71}Ge atom produced per day. After chemical extraction from the detector (Figure 10), ^{71}Ge is detected through the K capture reaction: $e^- + {}^{71}Ge \rightarrow {}^{71}Ga + \nu_e + X$ rays, whose half lifetime is $\tau_{1/2} = 11.4$ days (Figure 11). The first results come from an exposure period of 295 days and the observed solar neutrino flux is found to be: 83 ±19(statistical) ±8(systematic) SNU [17], which shows for the first time evidence of the production of pp neutrinos within the sun. The corresponding predictions from solar models are 131.5^{+7}_{-6} SNU (Bahcall) and 124 ± 5 SNU (Turck-Chièze); the details of the predictions are given in Table 2.

Table 2

Process	Bahcall	Turck-Chièze
$p\,p \rightarrow d\,e^+\,\nu$	70.8	70.6
$p\,e^-\,p \rightarrow d\,\nu$	3.1	2.8
$e^-\,^7Be \rightarrow\,^7Li\,\nu$	35.8	30.6
$^8B \rightarrow\,^8Be^*\,e^+\,\nu$	13.8	9.3
$^{13}N \rightarrow\,^{13}C\,e^+\,\nu$	3.0	3.9
$^{15}O \rightarrow\,^{15}N\,e^+\,\nu$	4.9	6.5
Total (SNU)	$\mathbf{131.5^{+7}_{-6}}$	$\mathbf{124 \pm 5}$

More data are expected from these two on-going experiments. In addition a confirmation of the good control of systematic errors should be obtained from calibrations with strong radioactive (10^6 curies) ^{51}Cr sources providing 750 keV neutrinos with a flux about five times the solar flux. The data from SAGE [18] (Figure 12) did not show a significant signal from solar neutrinos in a first stage but seem now to approach the results from GALLEX. More data and a final analysis are clearly needed to reach a definite conclusion.

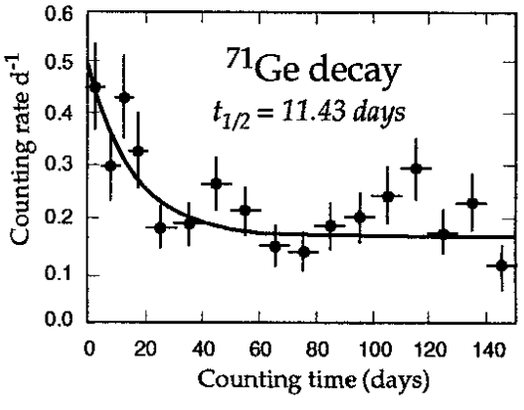

Figure 11 : Counting rate for ^{71}Ge extracted by GALLEX showing a half life of 11.43 days.

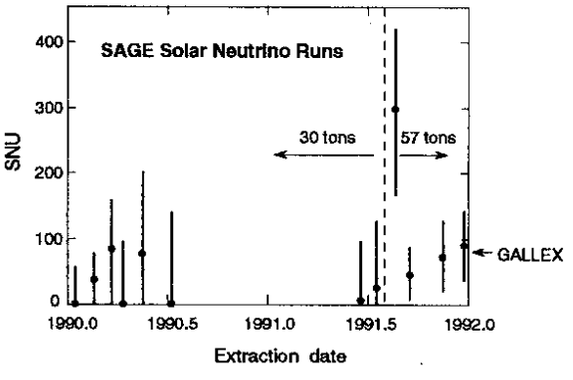

Figure 12 : Solar Neutrino Flux preliminary measurement by the SAGE experiment for the period 1990-1992.

The result of GALLEX, which is only two standard deviations below the SSM predictions, together with the results from Kamiokande II and Homestake does not eliminate the solar neutrino puzzle. The first natural question is to ask whether an astrophysical explanation is possible.

6.2 A cooler sun scenario

The principal uncertainties in the SSM are due to opacities. If the values used are overestimated, the core of the sun will be cooler and the production of high-energy neutrinos will be reduced. Since the effect of various possible nuclear and astrophysical explanations for the solar neutrino deficit is to lower the core temperature (T_c), it is reasonable to parametrize the various experimental results with T_c as a phenomenological parameter. The approximate correlations of the neutrino fluxes with T_c were obtained by Bahcall and Ulrich [11], and are given by simple power laws: $\Phi(pp) \sim T_c^{-1.2}$, $\Phi(^7Be) \sim T_c^8$ *and* $\Phi(^8B) \sim T_c^{18}$. For each experiment we can parametrize the rates relative to the SSM predictions as functions of T_c:

$$r_{Cl} = (1 \pm 0.033)\left[0.775 \times (1 \pm 0.100) \times T_c^{18} + 0.150 \times (1 \pm 0.036) \times T_c^{8} + \textit{small terms}\right]$$

$$r_{Kam} = (1 \pm 0.100) \times T_c^{18}$$

$$r_{Ga} = (1 \pm 0.04)\left[0.538 \times (1 \pm 0.002) \times T_c^{-12} + 0.271 \times (1 \pm 0.036) \times T_c^{18} + 0.105 \times (1 \pm 0.100) \times T_c^{18} + \textit{small terms}\right]$$

where T_c is the central temperature relative to the SSM ($T_c = 1 \equiv 15.67 \times 10^6$ K). The best fit requires lowering T_c by 5.5% with respect to the central value of the SSM prediction which is about a 2.5 standard deviation effect. Are 2.5 standard deviations a sufficient reason to exclude a cooler sun? Note that the fit becomes even better if, instead of Bahcall's, one uses the Turck-Chièze's model. On the other hand, can we neglect the sun model entirely? The larger Kamiokande rate relative to Homestake especially contradicts the T_c dependence of r_{Cl} and r_{Kam}. It would obviously be very nice if everybody were right and if there really was a 'Solar Neutrino Puzzle'. However, the best statement one can make at this stage is: if the SSM is right, then there is new physics in the neutrino sector.

6.3 The sun as the big neutrino 'regenerator' (MSW effect)

The sun's core has a very high density $\rho \sim 148$ g/cm^3, and in this very dense matter one must take into account the difference between ν_e and ν_μ in their interactions with matter. Neutral current processes are present for all neutrino species (ν_e, ν_μ and ν_τ), but charged current processes are present only for ν_e (Figure 13). This results in a different refractive index for ν_e and ν_μ in dense matter. This effect reminds us of the familiar K_L–K_S system. In dense matter the mass eigenstates are not simply described by:

$$\begin{pmatrix} \nu_1 \\ \nu_2 \end{pmatrix} = \begin{bmatrix} \cos(\theta) & -\sin(\theta) \\ \sin(\theta) & \cos(\theta) \end{bmatrix} \begin{pmatrix} \nu_e \\ \nu_\mu \end{pmatrix}$$

but by linear combinations with coefficients depending on the matter density. The effective mixing is modified by the presence of matter and, under certain conditions discovered by Mikheyev, Smirnov and Wolfenstein (MSW) [19], a resonance effect occurs (Figure 14).

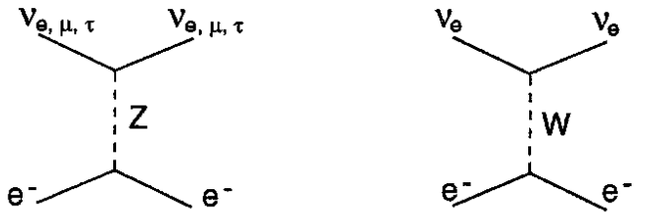

Figure 13 : Neutral and charged current interactions for neutrino on electrons in matter.

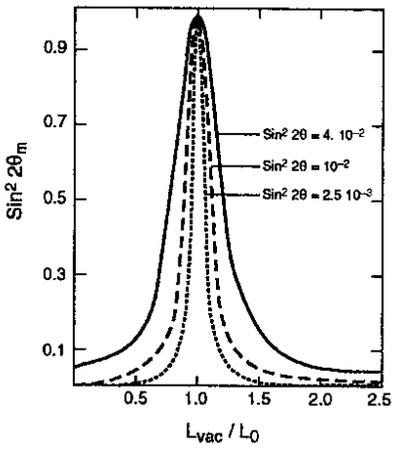

Figure 14 : Resonant behaviour of the mixing parameter for a $\nu_e \leftrightarrow \nu_\mu$ system in matter.

The initially small mixing angle becomes very large and, provided the variation of matter density near the critical value is not too abrupt (adiabaticity condition), there is almost complete ν_2 to ν_1 conversion. It is therefore possible that ν_e's produced in the sun's core go through a region of matter (Figure 15) where resonant conversion into ν_μ occurs as they travel towards us (Figure 16). Sterile neutrinos (ν_μ or ν_τ) which cannot be detected by inverse β-decay are produced and could explain the solar neutrino deficit observed by the experiments.

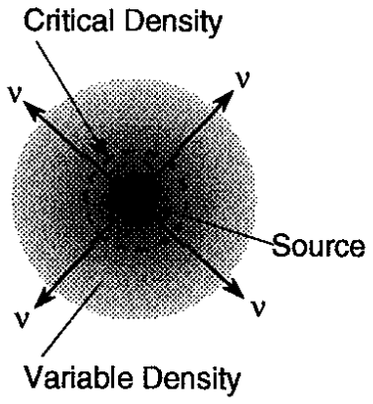

Figure 15 : Schematic representation of matter density in the Sun.

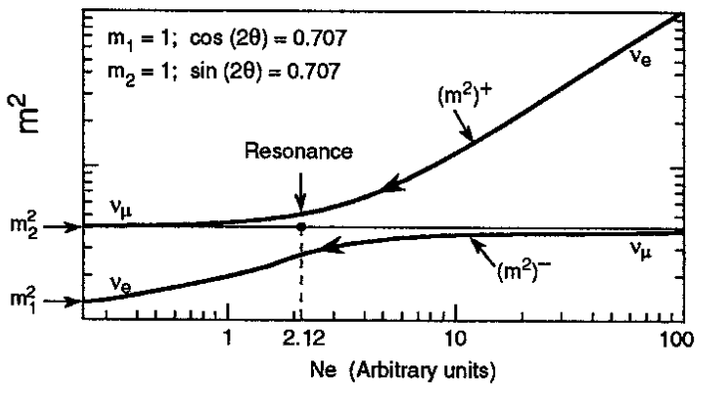

Figure 16 : Evolution of the mass eigenstates for a two-neutrino ($\nu_e \leftrightarrow \nu_\mu$) system as a function of electron density.

7 A POSSIBLE SCENARIO FOR NEUTRINO MASSES AND MIXING

Within the framework of the MSW effect, one can fit the solar neutrino experimental data to determine Δm^2 and $\sin^2(2\theta)$. One obtains two possible separate regions of the Δm^2 vs $\sin^2(2\theta)$ plane [20] (Figure 17): $\Delta m^2 \sim 10^{-5}$ eV^2 and $\sin^2(2\theta) \sim 10^{-2}$ or ≥ 0.6. The analogy with the CKM matrix for quarks suggests to exclude the solution with large mixing angle and to retain only: $\sin^2(2\theta_{ex}) \sim 10^{-2}$.

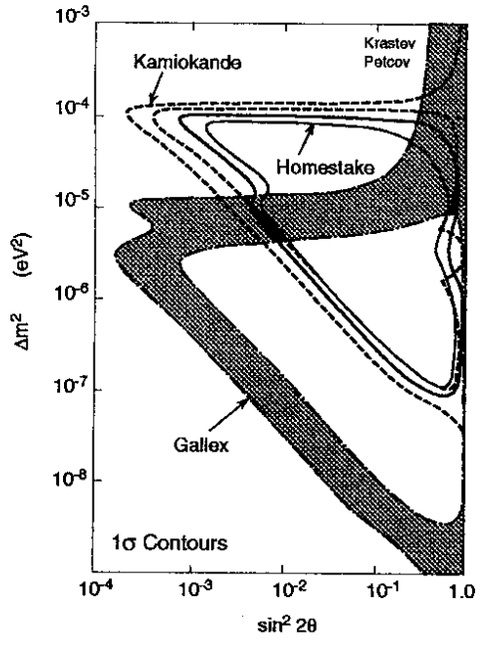

Figure 17 : MSW, 1 σ contours from solar neutrino experiments in the Δm^2, $\sin^2 2\theta$ plane, as computed by P.I. Krastev and S.T. Petcov [20].

Assuming $x = \mu$, and recalling the neutrino mass hierarchy that we expect in GUTs: $m_{\nu e} : m_{\nu\mu} : m_{\nu\tau} = m_u^2 : m_c^2 : m_t^2$, and using $m_u = 5$ MeV, $m_c = 1.5$ GeV and $m_t = 150$ GeV, we obtain: $\Delta m^2 \sim m_{\nu\mu}^2 = 10^{-5}$, which corresponds to $m_{\nu\mu} = 3 \times 10^{-3}$ eV. We can then use the see-saw mechanism to evaluate the other neutrino masses:

$$\frac{m_{\nu_\tau}}{m_{\nu_\mu}} = \left(\frac{m_t}{m_c}\right)^2 \sim 10^4 \Rightarrow m_{\nu_\tau} \sim 30\,eV$$

which is the order of magnitude needed to account for Hot Dark Matter. It is extremely intriguing that from pure particle physics considerations, we arrive at a value of the tau neutrino mass which is similar to the one obtained independently from cosmological considerations. The corresponding oscillation length for $\nu_\mu \leftrightarrow \nu_\tau$ is $\lambda = 2.75\ E_\nu$, where E_ν is in GeV and the oscillation length in metres. For example, a 20-GeV neutrino has an oscillation length of 55 metres.

Mixing angles can also be evaluated in a similar fashion: $\sin^2(2\theta_{\mu e}) = 10^{-2} \Rightarrow \sin^2(2\theta_{\mu\tau}) \sim 10^{-4}$. Mixing angles are indeed found to be very small. The present

experimental limit is $\sin^2(2\theta_{\mu\tau}) \leq 4 \times 10^{-3}$. The range down to 10^{-4} is experimentally observable, but this requires new experiments.

8 NEUTRINO OSCILLATIONS WITH COSMIC RAY NEUTRINOS

The atmospheric neutrinos are generated in decays of hadrons which are present in showers produced by primary cosmic ray interactions in the atmosphere. The production sequence is:

$$P+N \rightarrow \pi' s + K' s$$
$$\left(\pi^{\pm} / K^{\pm}\right) \rightarrow \mu^{\pm} + \left(\nu_{\mu} / \overline{\nu}_{\mu}\right)$$
$$\mu^{\pm} \rightarrow e^{\pm} + \left(\nu_{e} / \overline{\nu}_{e}\right) + \left(\overline{\nu}_{\mu} / \nu_{\mu}\right)$$

which means that one expects about twice as many muon neutrinos as electron neutrinos. Calculations of the neutrino fluxes [21] have an overall normalization error of about 20%, while the error on the ratio of ν_e and ν_μ is estimated to be only about 5%. The neutrino flux is approximately isotropic. Thus the total path length between the production point in the atmosphere and the detector varies from about 10 km to 13,000 km, depending on the zenith angle (Figure 18).

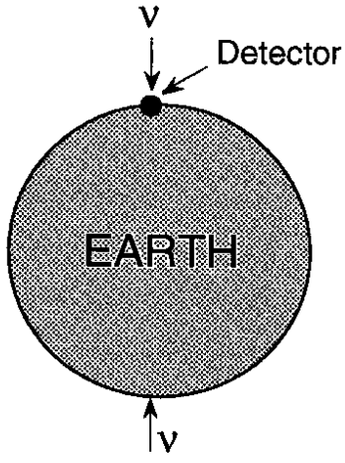

Figure 18 : Schematics of location of a neutrino experiment to study oscillations with atmospheric neutrinos.

In the presence of neutrino oscillations the detected neutrino fluxes will differ from the expected fluxes and one expects asymmetries in the up versus down rates at a given point on the earth. The measurement of atmospheric neutrino fluxes was pioneered by Kamiokande. Figures 19 a & b show the comparison of the data [22] with the calculation of ν_e and ν_μ events rates.

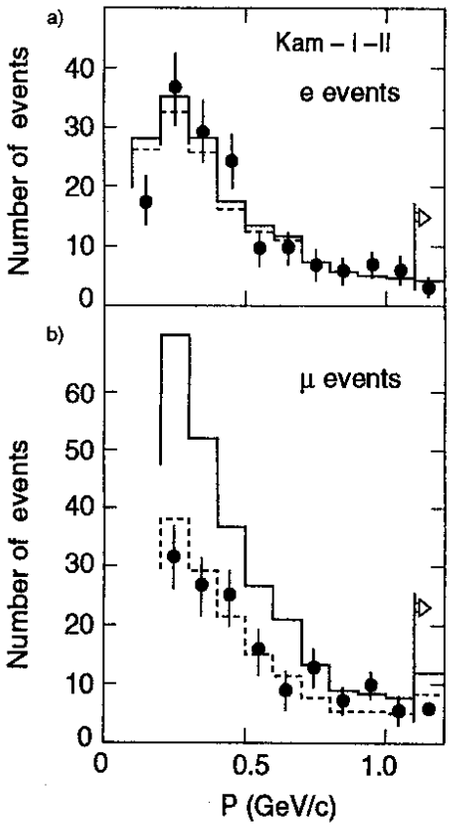

Figure 19: Kamiokande atmospheric neutrino data. (a) Momentum distribution of electron-like events; (b) : Momentum dis-tribution of muon-like events.

The solid histogram is the expected spectrum from Gaisser's calculations and the dashed histogram assumes oscillations with $\Delta m^2 = 8.10^{-3}$ eV^2, $\sin^2 2\theta = 0.87$.

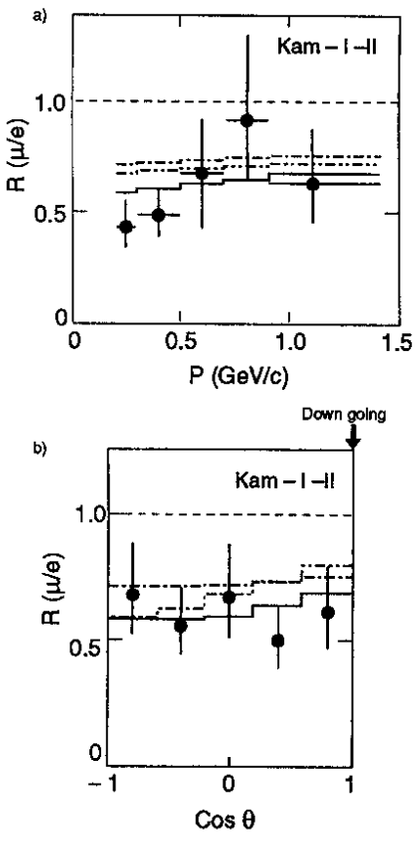

Figure 20: Kamiokande atmospheric neutrino data. (a) The variation of the ratio R as a function of momentum; (b) The variation of the ratio R as a function of the Zenith angle θ in Kamiokande. The solid, dash-dotted and dash-dot-dotted curves correspond to mixing with : (Δm^2, $\sin^2 2\theta$) = (8.10^{-3}, 0.87), (8.10^{-3}, 0.43) and ($1.1\ 10^{-3}$, 0.87) respectively.

While the electron events are consistent with the prediction, there is a large deficit of muon events which could be attributed to oscillations of ν_μ into ν_e or ν_τ. One can build a quantity which is less dependent on the overall normalization: $R \equiv R_{data}/R_{MC}$, where R_{data} is the ratio of μ-like to e-like events in the data, and R_{MC} is the ratio of μ-like to e-like events in the Monte Carlo sample. R is shown in Figure 20a as a function of momentum, and in Figure 20b as a function of zenith angle. Kamiokande obtains $R = 0.60^{+0.07}_{-0.06} \pm 0.05$ [22]. This is a rather large deficit. IMB-2 has also observed a deficit $R = 0.8 \pm 0.1$ [23], but only 2 standard deviations from 1. No evidence for ν_μ deficit was found by either the Frejus [24] or NUSEX [25] experiments. One could interpret this apparent deficit of ν_μ in atmospheric neutrinos as some evidence for $\Delta m^2 \sim 10^{-2}$ to 10^{-3} eV^2 but with a large mixing angle (Figure 21a & b). We can consider that the issue of atmospheric neutrino oscillations is still entirely open in view of the uncertainties in the predictions and of the preliminary character of the experiments.

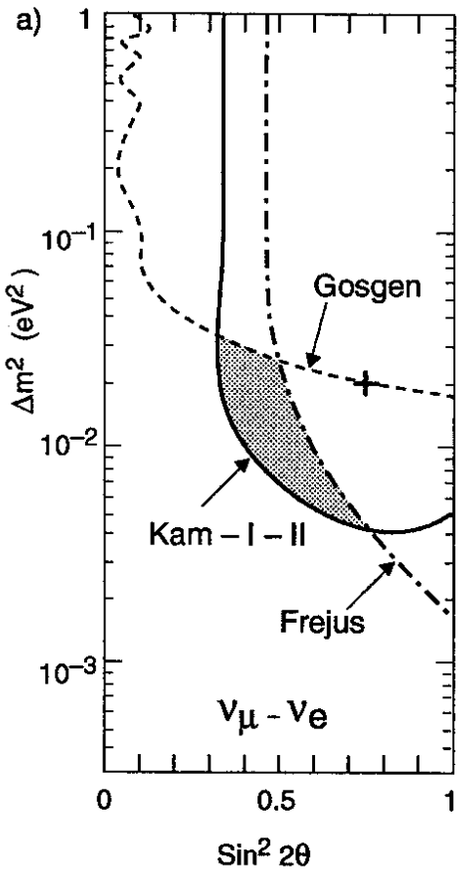

Figure 21a : Limits on Δm^2 versus $\sin^2 2\theta$ if Kamiokande atmospheric neutrino data are interpreted as oscillations between ν_μ and ν_e.

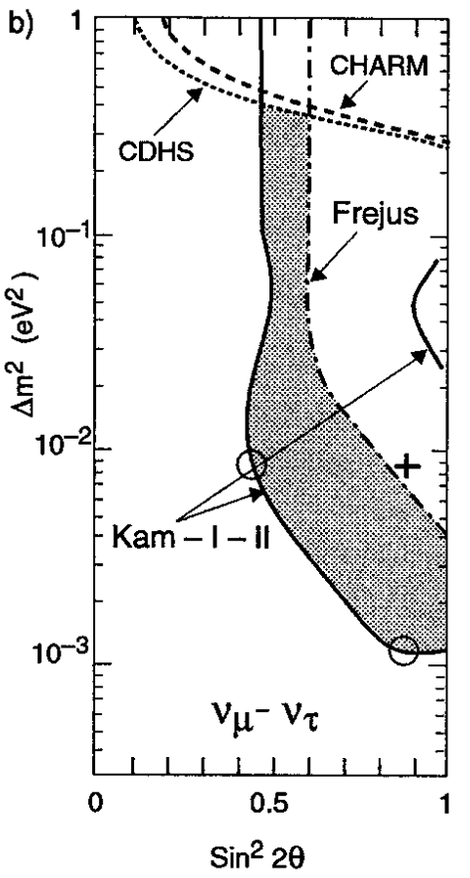

Figure 21b : Limits on Δm^2 versus $\sin^2 2\theta$ if Kamiokande atmospheric neutrino data are interpreted as oscillations between ν_μ and ν_τ.

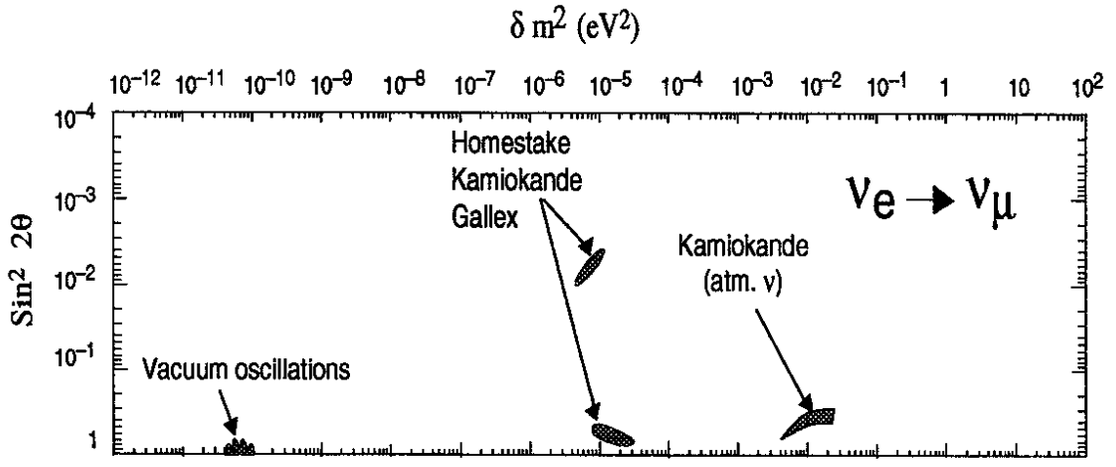

Figure 22 : Regions of the Δm^2 versus $\sin^2 2\theta$ plane allowed by solar and atmospheric neutrino data.

One can summarize the experimental status of neutrino oscillations experiments with the plot of Δm^2 versus the mixing parameter $\sin^2(2\theta)$ shown in Figure 22. There are four possible regions, one around $\Delta m^2 \sim 10^{-2}$ to 10^{-3} from atmospheric neutrinos, two around $\Delta m^2 \sim 10^{-5}$ from the MSW interpretation of solar

neutrino data, and one at $\Delta m^2 \sim 10^{-10}$ from the vacuum oscillation interpretation of solar neutrino data. A series of new experimental projects are in preparation which we expect will provide a definite answer to the matter of neutrino oscillations, and I propose now to review them in detail.

9 FUTURE EXPERIMENTAL PROJECTS

The main future projects are of two types: (1) search for $\nu_\mu \leftrightarrow \nu_\tau$ oscillations using a ν_μ accelerator beam; (2) study of solar neutrinos in large underground detectors also used to search for proton decay.

9.1 Search for $\nu_\mu \leftrightarrow \nu_\tau$ oscillations with the CERN ν_μ beam

In the CERN ν_μ beam, one expects that the relative fraction of ν_τ's produced directly from hadron decays (for instance $pN \rightarrow D_s$ + anything followed by $D_s \rightarrow \tau \nu_\tau$) should be smaller than 10^{-7}, therefore one can hope to detect ν_τ's produced from $\nu_\mu \leftrightarrow \nu_\tau$ oscillations down to a sensitivity of the same order. The neutrino beam is obtained from SPS protons in the West Area of CERN after rebuilding the entire neutrino beam line (Figure 23). There are currently two experiments scheduled to start data-taking in 1994. The first one is WA-95 known as CHORUS [26] from CERN **H**ybrid **O**scillation **R**esearch Apparat**US**. The CHORUS Collaboration have developed as part of their detector a system of 10^6 scintillating fibres. Their information is used to point tracks of selected events into the emulsion for computer-assisted search for ν_τ interactions (Figure 24). The signal for a τ decay in the emulsion is an apparent 'kink' in, for instance, a muon track extrapolated from the fibre information. The events to be measured are pre-selected with kinematical cuts.

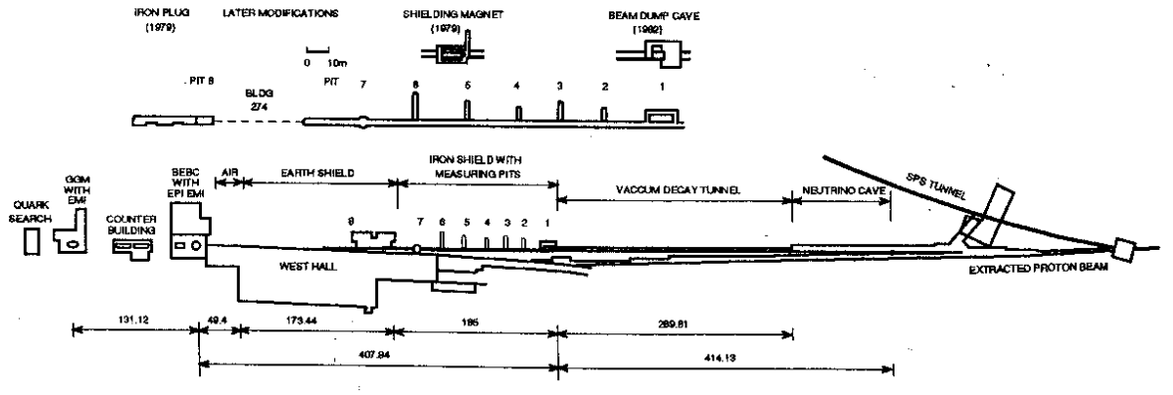

Figure 23 : The CERN west area SPS beam transport and neutrino beam facility for NOMAD and CHORUS.

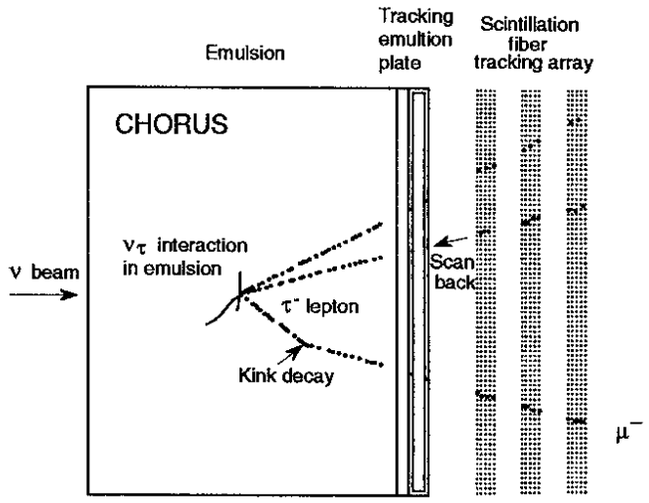

Figure 24 : Reconstruction of a ν_τ interaction in CHORUS.

The second experiment is WA-96 known as NOMAD [27] for Neutrino Oscillation MAgnetic Detector. NOMAD uses a complementary technique based on a very fine-grained target made of 150 drift chamber planes inside the magnet from UA1 (Figure 25). The extraction of a ν_τ signal is based on kinematical criteria. The beam is a practically pure ν_μ beam with only a small ν_e component. If ν_μ's oscillate into ν_τ's with a sufficiently high probability, ν_τ's would be found in the beam. The principle of the experiment is to search for ν_τ charged-current interactions producing a tau lepton observed in the detector. For instance: $\nu_\tau + N \rightarrow \tau^- +$ hadrons followed by $\tau^- \rightarrow \nu_\tau + h^-$, where $h^- = \pi^-, \rho^-, \pi^-\pi^-\pi^+$, or by $\tau^- \rightarrow \ell^- \nu_\tau \bar{\nu}_\ell$ etc.

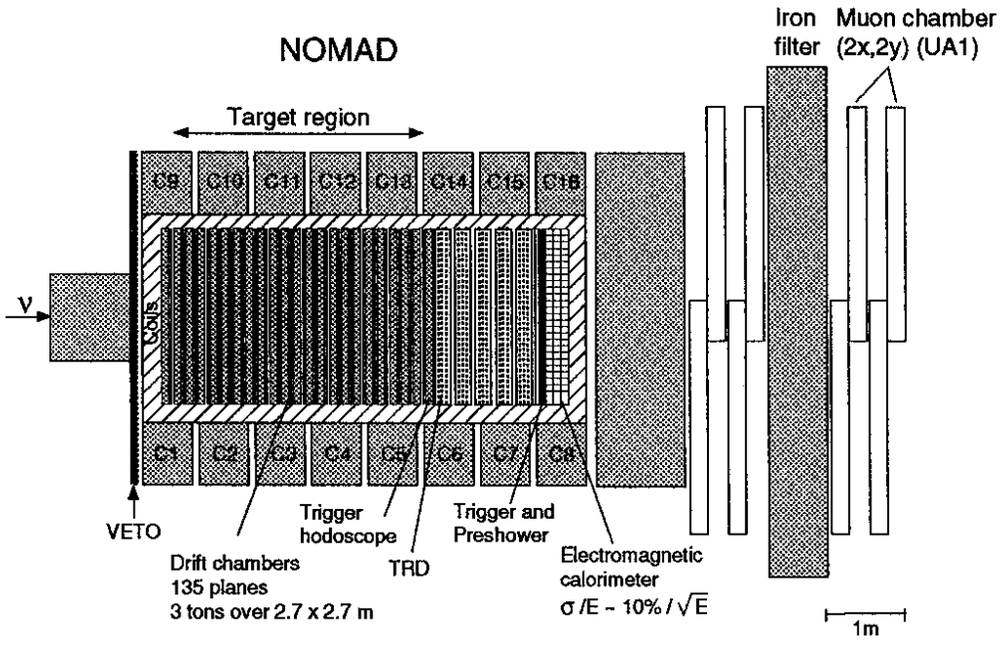

Figure 25 : Schematics of the NOMAD Detector.

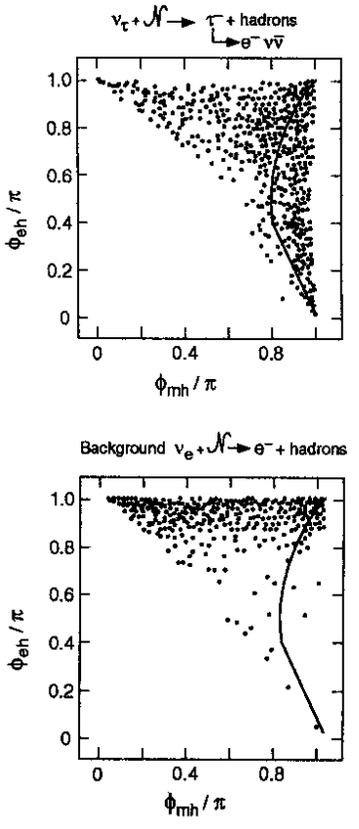

Figure 26 : Signal and background distributions of ϕ_{eh} the angle between the electron and the hadronic jet versus ϕ_{mh} the angle between the missing energy direction and the hadronic jet as computed by NOMAD. The angles are measured in the plane perpendicular to the initial neutrino direction.

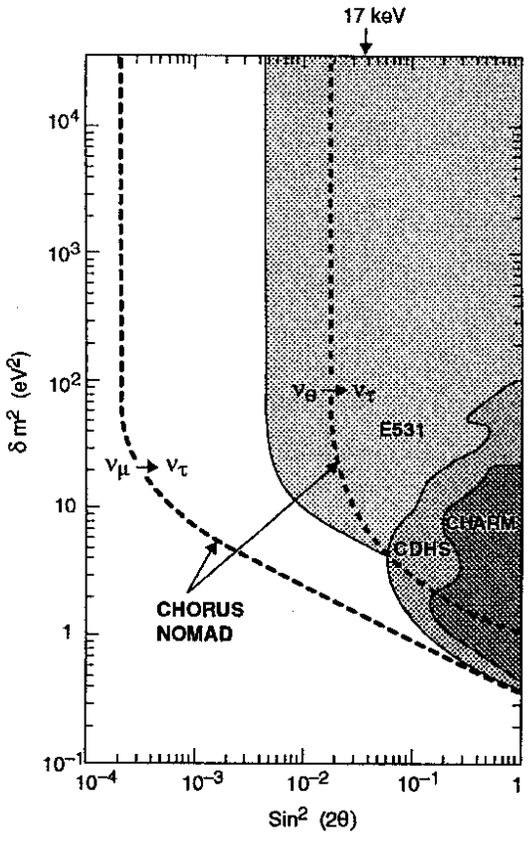

Figure 27 : Sensitivity of the CHORUS and NOMAD experiments for $\nu_\mu \leftrightarrow \nu_\tau$ and $\nu_e \leftrightarrow \nu_\tau$ oscillations.

The main background is hadrons faking a tau decay coming from the neutral-current process: $\nu_\mu + N \rightarrow \nu_\mu +$ hadrons, and which can be rejected by asking for large transverse momentum components $P_\tau > 1.6$ GeV and $P_{h^-} > 1.6$ GeV together with topological cuts requiring that the direction of the missing transverse energy in the event be away from the hadron jet, while the lepton or hadron produced in tau decay not be back to back with the hadron jet in the azimuthal angle direction (Figure 26).

Tables 3a and 3b show the details of the efficiency for the various τ decay channels considered, for CHORUS and for NOMAD respectively. The two experiments have similar sensitivity of $\sin^2(2\theta) \leq 3.5 \times 10^{-4}$ (90% C.L.). The combined CHORUS/NOMAD sensitivity should reach $\sin^2(2\theta) < 2.3 \times 10^{-4}$ for $m_{\nu_\tau} \geq 7$ eV, which is about 20 times better than the present limit (Figure 27).

Table 3a: CHORUS 5×10^5 ($\nu_\mu + N \rightarrow \mu^- +$ hadrons) events

Assume 1 event seen (from background) $\Rightarrow \sin^2 2\theta < 3.3 \times 10^{-4}$ (90% C.L.)

τ-Decay mode	Decay fraction	Efficiency	Events (signal) ($\sin^2 2\theta = 5.10^{-3}$)	Events (background)
$\nu_\tau \mu^- \bar{\nu}_\mu$	17.8%	8.4%	20	0.15
$\nu_\tau h^- + n\pi^0$	50%	4.0%	25	0.50
$\nu_\tau \pi^- \pi^+ \pi^-$	14%	5.5%	10	0.50
		TOTAL	55	1.15

Table 3b: NOMAD 1.1×10^6 ($\nu_\mu + N \rightarrow \mu^- +$ hadrons) events

Assume 7 events seen (from background) $\Rightarrow \sin^2 2\theta < 3.8 \times 10^{-4}$ (90% C.L.)

τ-Decay mode	Decay fraction	Efficiency	Events (signal) ($\sin^2 2\theta = 5.10^{-3}$)	Events (background)
$\nu_\tau e^- \bar{\nu}_e$	17.8%	13.5%	39	4.6
$\nu_\tau \mu^- \bar{\nu}_\mu$	17.8%	3.9%	11	2.2
$\nu_\tau \pi^- \pi^+ \pi^+ +$ n π^0	14%	7.7%	18	< 0.2
$\nu_\tau \pi^-$	11%	1.4%	3	< 0.2
$\nu_\tau \rho^- \rightarrow \nu_\tau \pi^- \pi^0$	21%	2.0%	7	< 0.2
		TOTAL	78	~ 7.0

An interesting possibility may exist to go down to $\sin^2(2\theta) \sim 10^{-5}$ by using the ICARUS detector technique of a liquid CH_4 time projection chamber in a 2-tesla magnetic field. A three-ton ICARUS prototype using liquid argon is currently working at CERN [28]. The idea here is to use the quasi-free protons provided by methane to completely determine the kinematics of ν_τ – proton collisions. With the additional constraint that the incident neutrino direction is known, using the energy and momentum conservation principle, one can determine completely the momentum of the outgoing neutrino in the case of a tau decay involving only one neutrino. One could then reconstruct invariant masses and the tau lepton would appear as a mass peak over a very low background reduced by cuts à la NOMAD. Such a technique under study applied to a 100-ton detector, may increase the sensitivity to $\nu_\mu - \nu_\tau$ mixing by one order of magnitude with respect to NOMAD and

CHORUS, thereby closing the window indicated by the MSW interpretation of solar neutrino data.

If Dark Matter is due to a massive ν_τ, the experiments described here could settle the issue, which would be a major milestone in our understanding of both the small-scale and the large-scale structure of our Universe.

9.2 Large underground experiments: Superkamiokande, ICARUS

One of the major future underground projects is Superkamiokande [29], in preparation in the same Kamioka Mine in Japan as Kamiokande and scheduled to start data-taking in 1996. The detector consists of 50,000 tons of water (Figure 28) and uses the same water Cherenkov light technique as Kamiokande. The useful fiducial mass, is 22,000 tons for proton decay and solar neutrino detection, and 32,000 tons for the detection of supernova neutrino bursts. The factor 15 to 30 increase in fiducial mass together with substantial improvements of the detector performance should make Superkamiokande a true second-generation experiment of great interest.

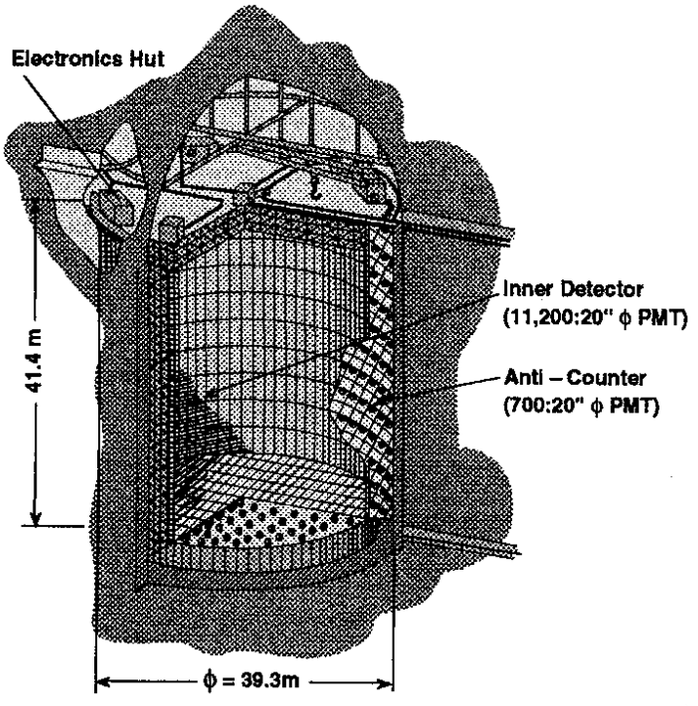

Figure 28 : Schematics of the Superkamiokande Detector.

The other major project is ICARUS [30] in preparation in the Gran Sasso Laboratory in Italy. The ICARUS programme consists of the construction and operation of three 5,000-ton liquid argon time projection chamber detectors (Figure 29), using ultra-pure argon technology and a new readout technique of ionization data over very large sensitive volumes, thereby providing 3-D imaging of any

ionizing event together with an excellent calorimetric response. The table 4 shows the detail characteristics of the ICARUS cryostat.

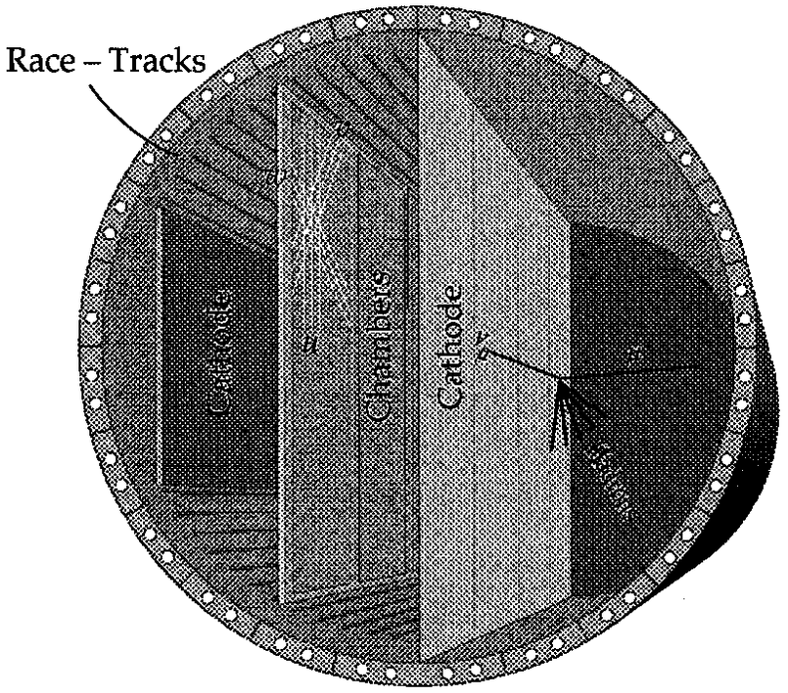

Figure 29 : Artist view of one 5,000 t ICARUS detector module at the Gran Sasso tunnel. The detector is symmetrical with respect to the central cathode plan.

Table 4: ICARUS CRYOSTAT PARAMETERS

	Internal vessel	External vessel
Shape	horizontal cylinder with domed ends	horizontal cylinder with flat ends
Diameter	16.0 m net	18.2 m external
Length	20.0 m net	24.8 m external
Volume	4,180 m^3 net, tot.	–
Filling ratio	0.90 to 0.95	–
Design pressure	0.2 MPa + hydro.	0.1 MPa external
Design temperature	85°K	20°C
Material	AISI 304 L	9% Ni steel
Hull structure	double, compart.	single, reinforced rings
Ends structure	double, compart.	sandwich, part. open
Body weight	~750 t total	~500 t total

A three-ton prototype has been operating successfully for more than one year at CERN [28] providing bubble-chamber-quality images of events (Figure 30a & b). The device is continuously sensitive and self-triggering. In a dedicated test with 5 GeV

pions at the CERN PS, using a 24 cm chamber with a 2 mm wire spacing, a space resolution of 60 μm was reached. The energy resolution is equally good : $\Delta E/E = 2.6\%/\sqrt{E} + 0.6$ % for electrons. ICARUS is designed to address a large variety of fundamental physics phenomena.

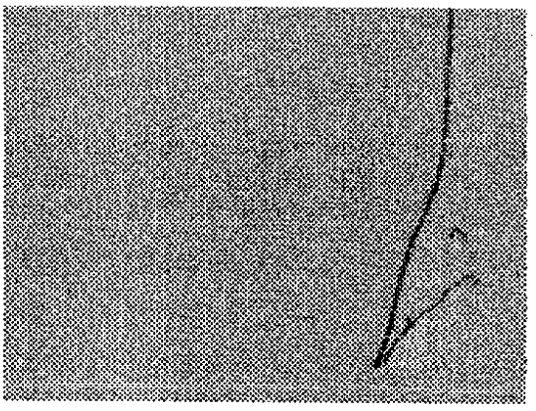

Figure 30a : Stopping muon event seen in the 3-ton ICARUS prototype at CERN. The gap between the muon and the electron tracks in this event corresponds to a time delay of 2.2 μs.

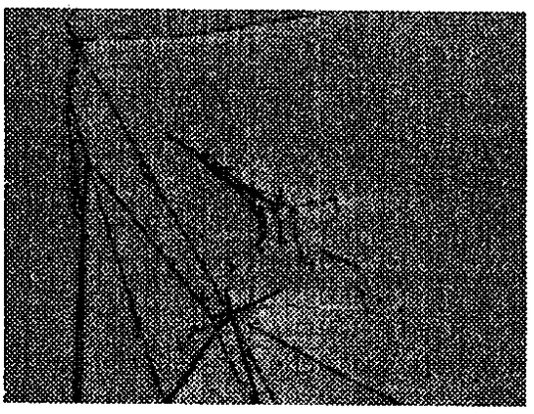

Figure 30b : Hadronic shower produced by a cosmic ray in the 3-ton ICARUS prototype at CERN.

(1) High-statistics, Solar Model independent study of solar neutrinos

The definitive study of the solar neutrino puzzle requires the simultaneous observation of $\nu_{e,\mu,\tau} + e \rightarrow \nu_{e,\mu,\tau} + e$ and of inverse β-decays in real time and with ample statistics. The reactions used by ICARUS for the direct observation of solar neutrinos from the ^8B cycle are: (1) $\nu_x + e \rightarrow \nu_x + e$ for which 2,900 events/year/module are predicted in the electron elastic channel assuming the Standard Solar Model rate and an efficiency of 69% for $E_e > 5$ MeV; (2) $\nu_e + {}^{40}Ar \rightarrow {}^{40}K^* + e$, a superallowed transition [31] followed by ($^{40}K^* \rightarrow {}^{40}K + 1$ or 2γ [2 MeV]) for which the Standard Solar Model predicts about 2400 events/year/module including 70% detection efficiency assumed in ICARUS for $E_e > 5$ MeV.

The distinctive properties of the recoil electron energy spectrum together with the detection of photon energy associated with the $^{40}K^*$ decay allow one to measure the ratio R of elastic electron scattering to absorption cross-sections (Figure 31). This ratio provides a direct measurement of the fraction of ν_e's which converted to ν_μ's or ν_τ's through oscillations.

With one year of data ICARUS can separate the present two Mikheyev–Smirnov–Wolfenstein (MSW) solutions by 10 standard deviations (statistical). The sensitivity region shown indicates that after one year ICARUS could detect a 5% departure from the central value of the Standard Solar Model prediction (Figure 32).

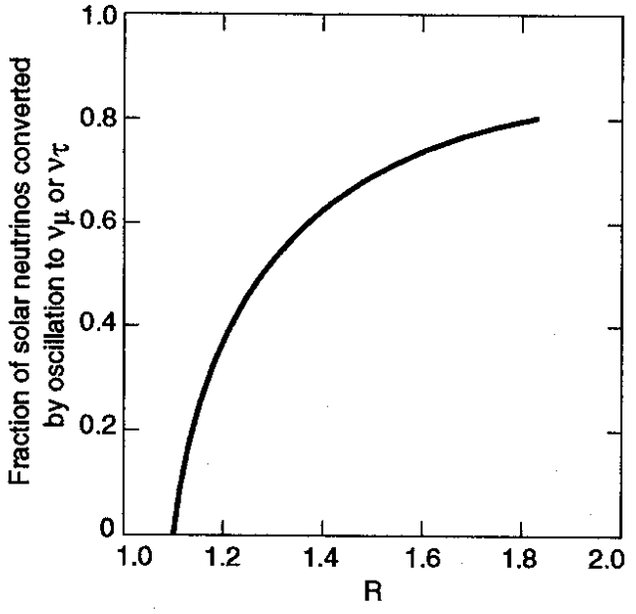

$$R = \frac{N(\nu_e + e^- \rightarrow \nu_e + e^-) + N(\nu_{\mu,\tau} + e^- \rightarrow \nu_{\mu,\tau} + e^-) \cdot \dfrac{\sigma(\nu_\mu e^- \rightarrow \nu_\mu e^-)}{\sigma(\nu_e e^- \rightarrow \nu_\mu e^-)}}{N(\nu_e + {}^{40}Ar \rightarrow e^- + {}^{40}K^*)}$$

Figure 31 : The ratio R as a function of the fraction of ν_e's from the sun which converted to ν_μ's or ν_τ's. The SSM corresponds to R = 1.1.

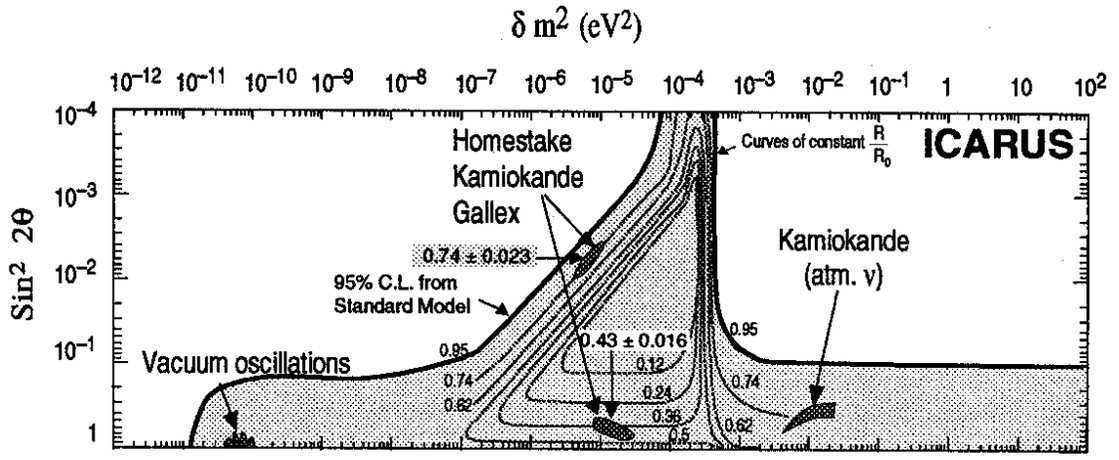

Figure 32 : Sensitivity of the ICARUS experiment for solar neutrinos, corresponding to one year of data. The curves represent constant values of the ratio R/R_O. Where R is the ratio of the neutrino absorption to elastic cross-section and R_O = 1.1.

(2)High-statistics study of atmospheric neutrinos

The full event reconstruction capability of ICARUS allows a precise and unambiguous measurement of upward- versus downward-going neutrinos, with large statistics. In particular the excellent e/μ separation in ICARUS and precise energy measurement provide an accurate reconstruction of the neutrino energy

spectrum and flavour composition. ICARUS can detect neutrino interactions down to a few MeV. The total number of charged-current events expected for atmospheric neutrinos, in 2π steradians, assuming no oscillations, is of the order of 600 per year per module using the flux calculation from T. Gaisser et al [21]. The flavour composition of down-going neutrinos is expected to be approximately 35% ν_e and 65% ν_μ. The high statistics will allow studies of baseline variations from angular distributions. The expected Δm^2 sensitivity should at least extend down to 10^{-4} eV^2.

(3) Search for nucleon decay up to lifetimes approaching 10^{34} years

Precision measurements of coupling constants at LEP have shown that the unification of forces does not occur naturally in the Standard Model (curves miss by 9 standard deviations). However, in the framework of the Minimal Supersymmetric Model, unification is possible and the unification scale is of the order 10^{16} GeV. The proton decay issue is therefore still entirely open.

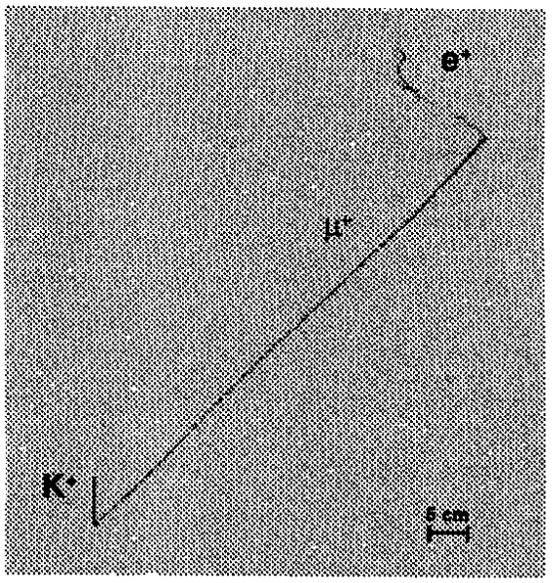

Figure 33a : Simulation of a proton decay $p \rightarrow K^+\nu$ in ICARUS.

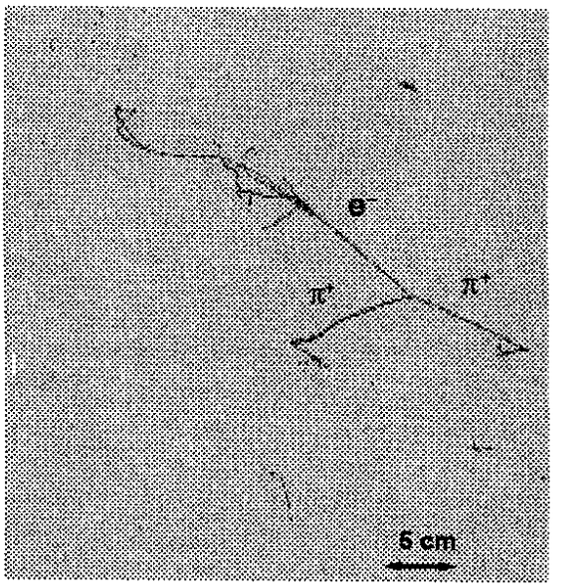

Figure 33b : Simulation of a proton decay $p \rightarrow e^-\pi^+\pi^+$ in ICARUS.

With ICARUS and a sensitive mass of 4,700 tons per module, many exclusive channels can be searched for simultaneously. In addition, the possibility of using a CERN neutrino beam aimed at Gran Sasso provides a unique tool to calibrate the background. Within one year ICARUS will either reach or exceed all world limits, and, depending on the number of modules built, will probe part or most of the lifetime region between 10^{33} and 10^{34} years in more than 10 different decay channels. The simulation of some of the proton and neutron decay events shown (Figure 33a, b & c) indicates clearly that, with the good energy resolution (Figure 34) and particle

identification of ICARUS, nucleon decays will be observed with an exceedingly small residual background from neutrino interactions.

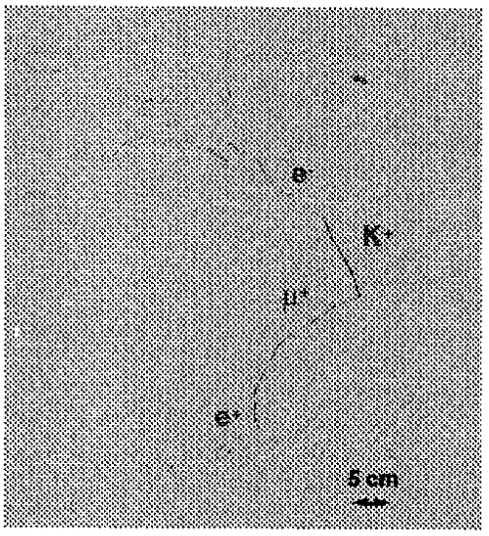

Figure 33c : Simulation of a neutron decay $n \rightarrow e^- K^+$ in ICARUS.

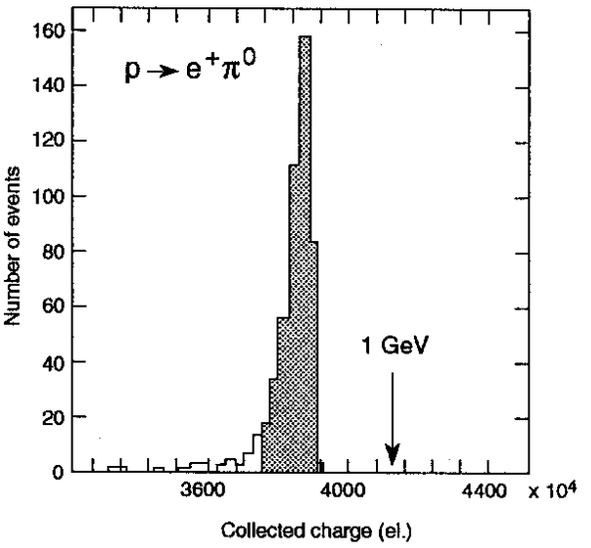

Figure 34 : Simulation of the total charge collected in ICARUS for proton decays in the $p \rightarrow e^+\pi^0$ channel.

9.3 Long-range accelerator neutrinos

One interesting possibility to increase the sensitivity of accelerator neutrino oscillation experiments is to extend the baseline outside the limits of the laboratory. A feasibility study [32] has shown that it is possible to send a CERN ν_μ beam to Superkamiokande or to Gran Sasso. Figure 35 shows the depths reached by various possible CERN beams. The azimuthal view (Figure 36) shows that at CERN both Gran Sasso and Superkamiokande are in a favourable direction, that is where an SPS proton beam already exists in the right direction. DUMAND requires a slope for the beam of 57 degrees which makes it technically very difficult. Gran Sasso and Superkamiokande are therefore the preferred solutions.

Neutrino beams offer several clear advantages:

- The energy spectrum is more sharply peaked and better known than for atmospheric neutrinos.
- The energy can be tuned.
- One can switch between neutrinos and anti-neutrinos (interesting for matter effects).
- Known direction and timing allow efficient background rejection.

- Known initial beam composition (almost entirely ν_μ or $\bar{\nu}_\mu$).
- High rate for statistical accuracy.
- As most neutrino detectors are also proton decay detectors, an accelerator neutrino beam can be used to calibrate the neutrino background to proton decay by providing neutrinos of the appropriate energy.

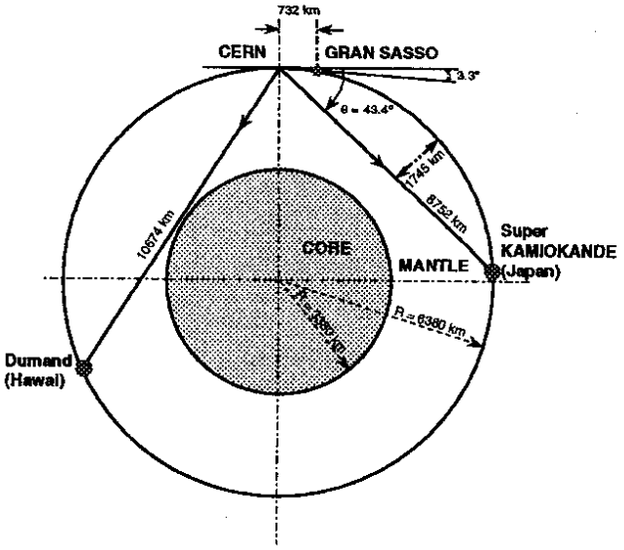

Figure 35 : Various possibilities of neutrino beams from CERN towards existing large neutrino detectors.

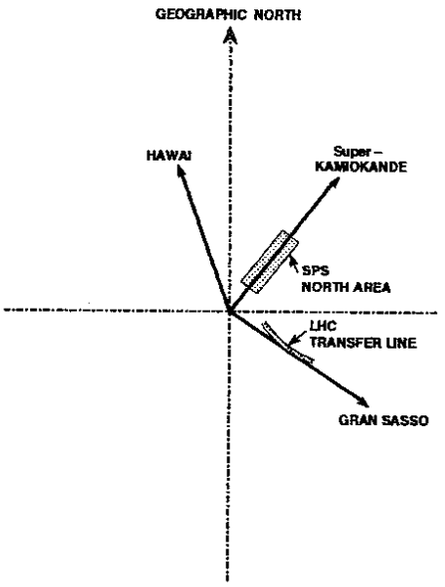

Figure 36 : Azimuthal directions at CERN of Dumand, Superkamiokande and ICARUS.

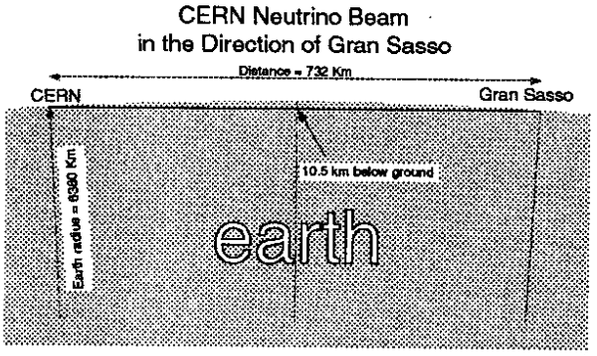

Figure 37 : Schematic cross-section of the Earth showing the CERN neutrino beam in the direction of Gran Sasso.

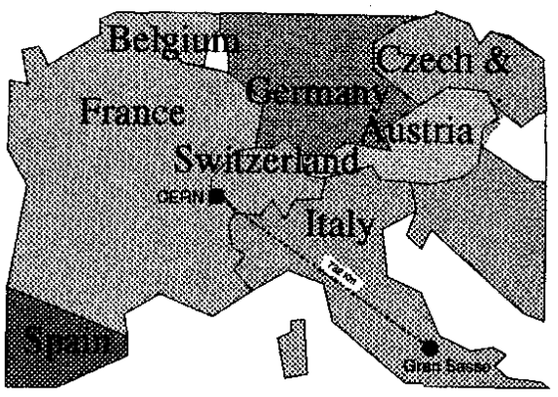

Figure 38 : Geographic map showing the path of the CERN neutrino beam in the direction of Gran Sasso.

The profile of the beam to Gran Sasso is shown in Figure 37. It goes under three countries: France, Switzerland and Italy (Figure 38). The optimal conditions with ICARUS are obtained with 80-GeV protons from the CERN SPS (2×10^{13} protons on target every 2.4 s) mainly due to the fact that the π^0 background increases with

energy. There are two main types of background to charged-current interactions of a genuine ν_e coming from a ν_μ oscillation:

(i) ν_e in the initial beam: they mostly come from K decays. Because their transverse momentum is larger than ν_μ coming from π decays, as the distance increases their proportion decreases, and at Gran Sasso they are practically negligible for 80-GeV protons (2.5×10^{-4}).

(ii) Neutral-current interactions of ν_μ producing a recoiling jet with π^0's faking electrons (~ 1.5 π^0/jet). In ICARUS π^0's can be identified from their decay properties (separation of the photon showers), from the shape of the shower, and from ionization information. A detailed Monte Carlo simulation has shown that the π^0 background can also be made practically negligible in the 80-GeV proton case ($\leq 0.1\%$).

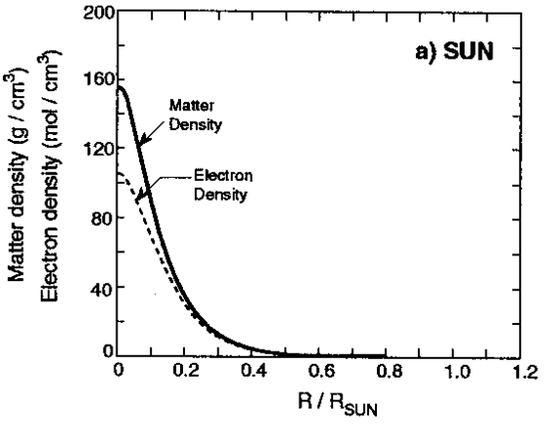

Figure 39a : Matter and electron density in the Sun as a function of the distance to the center.

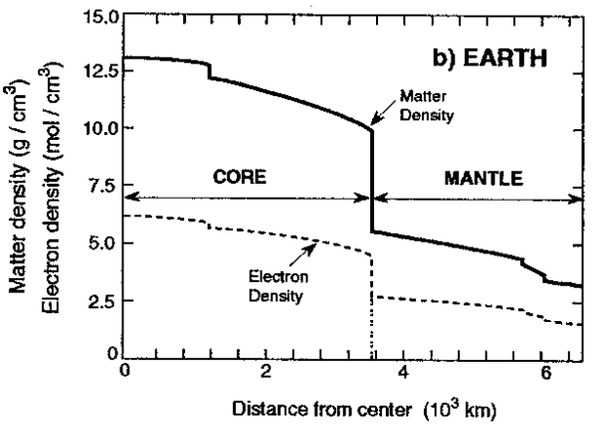

Figure 39b : Matter and electron density in the Earth as a function of the distance to the center.

In the case of Superkamiokande, in addition to vacuum oscillations there also exists the possibility to study matter effects, so crucial in our understanding of solar neutrinos. While the matter density at the centre of the sun is more than one order of magnitude larger than at the centre of the earth (Figure 39a & b) the average matter density in the earth ($5.5 g/cm^3$) is five times larger than in the sun. If matter effects exist in the sun, they should also occur in the earth. For a neutrino beam going through the centre of the earth, the resonance spectrum in the conversion of ν_μ into ν_e is dominated by two main structures, the effect of the earth's core and the effect of the earth's mantle (Figure 40) [33]. In Superkamiokande's case, since the beam does not go through the core, the main resonant structure is the one corresponding to $\Delta m^2/E = 0.5$, a value fairly independent of the chosen value of $\sin^2(2\theta)$ (Figure 41). For Gran Sasso, unfortunately, the neutrino path in matter is insufficient to reach a spectacular resonance (Figure 42) [34].

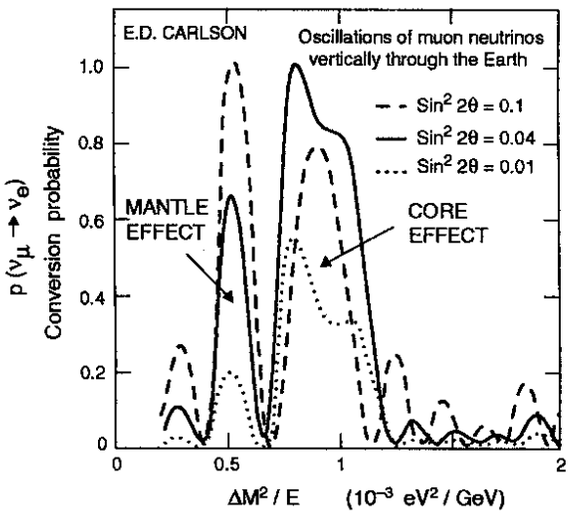

Figure 40 : Matter oscillation pattern for neutrinos going through the Earth vertically through the center [33].

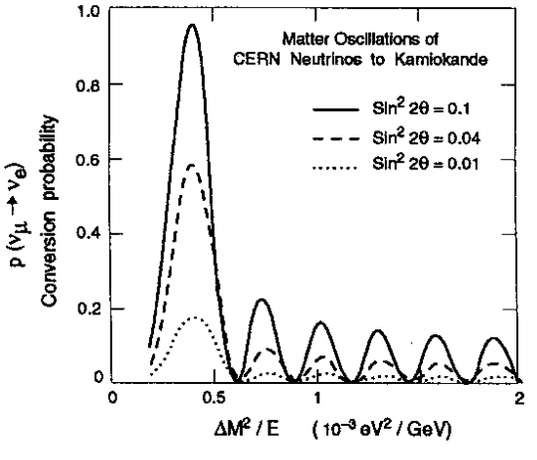

Figure 41 : Matter oscillation pattern for neutrinos travelling in the Earth from CERN to Superkamiokande.

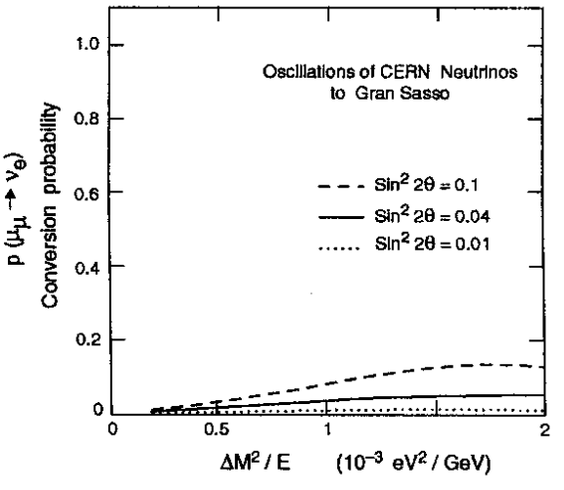

Figure 42 : Matter oscillation pattern for neutrinos travelling in the Earth from CERN to Gran Sasso.

Assuming that one uses CERN neutrino beams from protons of 80 to 450 GeV, one obtains a large sensitivity region of Superkamiokande, shown in Figure 43, which largely covers the present atmospheric neutrino solution. Figure 43 also shows that for vacuum oscillations, Superkamiokande would reach $\Delta m^2 \sim 10^{-4}$ eV^2 for full mixing. However, one should note that the sensitivity regions derived here assume no background in Superkamiokande. The effective sensitivity will have to be determined with full simulation of the detector. Our purpose here is simply to point out the unique potential of a CERN neutrino beamline to Japan. If such matter effects

were to be observed with neutrinos, a straightforward consistency check will be to verify that the effects disappear for antineutrinos or vice versa.

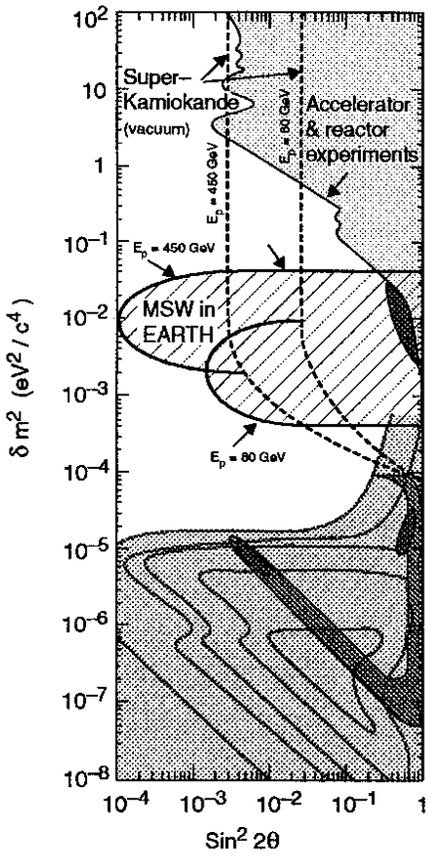

Figure 43 : Sensitivity in the Δm^2 versus $\sin^2 2\theta$ plane of neutrino oscillations in vacuum and in matter for neutrinos from CERN to Superkamiokande.

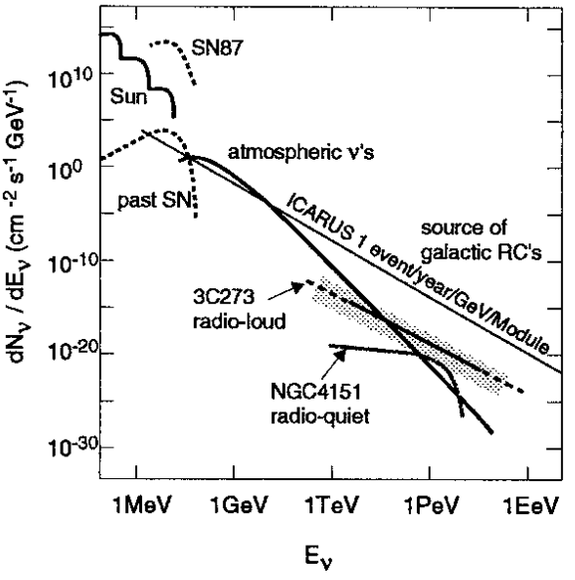

Figure 44 : Distribution of the energy of neutrinos for various astrophysical sources : Sun, Supernova, cosmic rays, etc. The sensitivity of ICARUS is indicated.

9.4 Astrophysical and cosmological studies

There are several classes of astrophysical and cosmological phenomena that can be studied with a neutrino telescope such as ICARUS.

(i) In addition to the study of intrinsic neutrino properties, solar neutrinos obviously constitute a window for the understanding of neutrino production mechanism inside stars. The electron recoil energy distribution for elastic scattering and absorption events and their fluxes will provide direct information on ^{8}B solar neutrinos.

(ii) Search for neutrino bursts from supernova collapses (galactic, extra galactic) and for relic supernova neutrinos will provide important new constraints on models. The search for new sources of low-energy neutrinos or antineutrinos uses the reaction: $\nu_x\ e \rightarrow \nu_x\ e$ where x stands for any type of neutrino or antineutrino. A

practical threshold is $E_e \geq 5$ MeV to be compared with the energy of supernova neutrinos above 10 MeV. There is a unique energy window above the solar ^8B neutrinos and below cosmic neutrinos (Figure 44) where one could detect neutrinos coming from all supernovae which occurred in the history of the Universe. These neutrinos are expected to be red-shifted but not thermalized. If such a signal were to be found one would gain new information on baryonic matter in our Universe.

ICARUS should therefore open a new window in our understanding of the Universe and of its 'Big Bang' origin.

10 CONCLUSION

We are witnessing a renaissance of experimental neutrino physics because solar neutrino and perhaps also atmospheric neutrino experiments give us a hint of new phenomena, beyond the present Standard Model.

New detectors with larger fiducial volumes and more powerful detection techniques are in preparation for solar neutrinos studies, high-sensitivity searches for $\nu_\mu \leftrightarrow \nu_\tau$ oscillations and for long-baseline ν_μ oscillations studies. These new experiments will definitely assess the issues of neutrino mixing and of neutrino masses with their possible important cosmological implications.

There is a definite hope for new exciting results on the subject before the end of this century.

11 REFERENCES

[1] T. Yanagida, Progr. Theor. Phys., B 135 (1978) 66; M. Gell-Mann, P. Ramond and R. Slansky, in *Supergravity*, eds. P. van Nieuwenhuizen and D. Freedman (North Holland, Amsterdam 1979), p. 315.

[2] S. Bludman, D. Kennedy and P. Langacker, *Nucl. Phys.* B374, 373 (1992); Phys. Rev. D45, 1810 (1992).

[3] P. Langacker and M.X. Luo, *Phys. Rev.* D44, 817 (1991).

[4] P. Langacker et al., *Nucl. Phys.* B282, 589 (1987).

[5] E.W. Kolb and M.S. Turner, *The early universe* (Addison-Wesley, Menlo Park, CA, 1990) ch. 1, 3 and 5; S.A. Bludman, CfPA (Berkeley) preprint CfPA-TH-91-004 (1991).

[6] L. Rolandi, *"Precision Tests of the Electroweak Interaction"*, Proc. of International Conference on High Energy Physics, 1992, Dallas, Texas, USA.

[7] D. Kazanas, *Astrophys. J.*, 241 (1980) L59; A. Guth, *Phys. Rev.*, D23 (1981) 347.

[8] G.F. Smoot et al., Astrophys. J. 396, 3, 155-B5 (1992); G.F. Smoot et al., Astrophys. J. 396, L1, 160-B1 (1992); G.F. Smoot et al., COBE preprint (1992); E.L. Wright et al., COBE preprint (1992).

[9] Davis, Jr., R., BNL50879, *The Status and Future of Solar Neutrino Research*, 1, (1978), G. Friedlander, Editor.

[10] R. Davis, Workshop on Neutrino Telescopes, ed. M. Baldo-Ceolin, Palazzo Loredan, Venice, Feb. 1990, p. 1-13.

[11] J.N. Bahcall, Review talk to Neutrino '90 Conf., CERN, June 1990 [Nucl. Phys. Proc. Suppl. B19 (1991)]; J.N. Bahcall, *Sci. Am.* (June 1990), p. 26; J.N. Bahcall and R.K. Ulrich, *Rev. Mod. Phys.*, 60 (1989) 297; J.N. Bahcall and Pinsonneault, *Rev. Mod. Phys.*, 64, (1992) 885.

[12] S. Turck-Chieze et al., *Astrophys. J.* 335 (1988) 4415; S. Turck-Chieze, Proc. Int. Conf. 'Inside the Sun', Versailles, 1989, eds. G. Berthomieu and M. Cribier (Kluwer Acad. Publ., Dordrecht 1989), p. 125.

[13] K.S. Hirata et al., *Phys. Rev. Lett.* 65, 1297 (1990); *Phys. Rev. D* 44, 2241 (1991); M. Takita, Doctor Thesis, Univ. of Tokyo (Feb. 1989), ICR Report 186-89-3; K. Kihara, Doctor Thesis, Univ. of Tokyo (March 1992), ICR-Report 274-92-12.

[14] M. Mori, Workshop on Neutrino Telescopes, ed. M. Baldo-Ceolin, Palazzo Loredan, Venice, Feb. 90, p. 1-13; K.S. Hirata et al., *Phys. Rev. Lett.* 65 (1990) 1297.

[15] The SAGE Collaboration, "First results from the Soviet-American Gallium Experiment", Neutrino '90, Proceedings of the 14th International Conference on Neutrino Physics and Astrophysics, CERN, Geneva, Switzerland, 10-15 June 1990, *Nucl. Phys. B* (Proc. Suppl.) 19 (1991) 84-93.

[16] T. Kirsten, "The GALLEX Project of Solar Neutrino Detection", *Adv. Nucl. Astrophys.* (Editions Frontières, 1986) pp. 85-96.

[17] P. Anselmann et al., *Phys. Lett.* B285, 376 & 390 (1992).

[18] A.I. Abazov et al., *Phys. Rev. Lett.* 67, 332 (1991); V.N. Gavrin et al., Proceedings, XXVI International Conference on High Energy Physics, Dallas, Texas, USA (1992).

[19] L. Wolfenstein, *Phys. Rev.* D17, 2369 (1978); D20, 2634 (1979); S.P. Mikheyev and A.Yu. Smirnov, *Yad. Fiz.* 42, 1441 (1985); *Nuo. Cim.* 9C, 17 (1986); H. Bethe, *Phys. Rev. Lett.* 56 (1986), 1305.

[20] P.I. Krastev & S.T. Petcov, CERN TH 6539 (1992), sumitted to *Phys. Lett. B.*

[21] G. Barr, T. Gaisser and T. Stanev, *Phys. Rev.* D39 (1989) 3532.

[22] K.S. Hirata et al., Phys. Lett. B280 (1992) 146-152.

[23] D. Casper et al., *Phys. Rev. Lett.* Vol 66 (1991) 2561.

[24] Ch. Berger et al., *Phys. Lett.* B227 (1989) 489; *Phys. Lett.* B245 (1990) 305.

[25] M. Aglietta et al., *Europhys. Lett.* 8 (1989) 611.

[26] CHORUS Collaboration, N. Armenise et al., CERN-SPSC/90-42 (1990).

[27] NOMAD Collaboration, P. Astier et al., CERN-SPSLC/91-21 (1991), CERN-SPSLC/91-48, SPSLC/P261 Add. 1.

[28] P. Cennini et al., *"A three ton liquid argon time projection chamber"*, to be submitted to Nuc. Inst. Meth.

[29] M. Koshiba, Proc. of Workshop on Grand Unified Theories and Cosmology, KEK, Japan, December 1983, P24; Y. Totsuka, Proceedings of the Seventh Workshop on Grand Unification / ICOBAN '86, April 1986, Toyama, Japan, P78; A. Suzuki, Proc. of the Workshop on Elementary Particle Picture of the Universe, KEK, Japan, February 1987, P136.

[30] CERN - Harvard - Milano - Padova - Roma - Tokyo - Wisconsin Collaboration, INFN/AE-85/7, Frascati (1985); C. Rubbia, CERN-EP Internal Report 77-8 (1977); ICARUS Collaboration, ICARUS I : An Optimized Real Time Detecor of Solar Neutrinos, LNF-89/005 (R) (1989).

[31] J.N. Bahcall, M. Baldo-Ceolin, D. Cline, and C. Rubbia, Phys. Lett. B178 (1986) 324; R.S. Raghavan, Bell Labs, T.M. 79-1131-31 (79) unpublished.

[32] A. Ball et al., CERN-SL note 92-75 (B5).

[33] E.D. Carlson, *Phys. Rev.* D34, 1454 (1986).

[34] P.I. Krastev and F. Cavanna, Private Communication.